Figure 1 Langerhans cell histiocytosis skin lesions and systemic positron emission tomography imaging. A: Soft papular skin lesion is found at the inguinal area. Biopsy of the lesion revealed the histology of langerhans cell histiocytosis; B, C: Positron emission tomography scan shows multiple lesions, at the scapulas, plevic bones, cervical and inguinal lymph nodes: frontal view (B), lateral view (C).

masses (at her left upper arm and elbow). The lesions at the Th3-4 caused paresis due to spinal compression, which needed laminectomy. She was initially treated with bisphosphonate alone, but thereafter with intensive systemic chemotherapy (JLSG-96 protocol)[13], including vincristine and cytosine arabinoside. However, 2 years later, she needed allogeneic hematopoietic stem cell transplantation (HSCT) because of progressive disease. The patient has currently been alive without active disease (ASAD).

Case 4

A 37-year-old male was found to have CDI, in association with hyper-prolactinemia (seum PRL 56.1 ng/mL). A thickened pituitary stalk was demonstrated on brain magnetic resonance imaging (MRI), which biopsy revealed LCH. Since then he developed multiple bone lesions at spines (cervical, lumbar), bilateral ilium, left sacroiliac joint, and bilateral ribs as well as skin lesions (Figure 1A) and cervical lymphadenopathy. He was treated first with PSL and bisphosphonate followed by systemic chemotherapy (JLSG-96 protocol)[13]. One year later, because of progression of the disease (Figure 1B and C), he received HSCT and has currently been in a state of ASAD.

Case 5

A 40-year-old male complained first of mandibular pain. He was found to have multiple bone lesions (left man-

dible, left temporal, occipital, bilateral femurs, cervical spines and right petrous bone. Biopsy of the temporal bone lesions revealed LCH. He was treated with irradiation (6 Gy) to the left petrous bone and systemic chemotherapy, including vinblastine (VBL) and PSL followed by the JLSG-96 protocol[13] and bisphosphonate; however, reactivation occurred to C1, C2, right mandible, Th5, bilateral femur distal end. Thereafter, he responded well to the chemotherapy with 2-deoxychloroadenosine (2CDA; cladribine). The patient has currently been in a state of ASAD.

Case 6

A 46-year-old female, who was first noted to have thyroid cysts at age 43, complained of back pain and found to have a compression fracture of Th4. A year later she complained of right rib pain. Positron emission tomography (PET) scan revealed hot spots (SUVmax; 7.0) at the both thyroid lobe (Figure 2A) as well as other numerous hot spots at the deep cervical lymph nodes, right scapula, right ilium as well as right rib. Another year later, right lobe of the thyroid was removed, which was diagnosed as LCH. She also received a resection of right rib, which was also found to be LCH. Since then, she was treated with VBL and PSL; however, treatment was stopped because of VBL neurotoxicity. Thereafter, new bone lesions at the frontal bone, rib, ankle, knee, *etc*. She gave births two children; however, the initiation of LCH was not relevant to her childbirth. The patient has continued to have active disease (alive with active disease, AWAD).

Case 7

A 40-year-old male complained of nuchal and left-shoulder pain without any triggering events. With MRI, he was found to have a mass at the left upper and lower articular processes and part of the left articular arch of C3, which was positive for Ga[67] bone scintigraphy. This mass was totally resected. Nearly 2 years later, he had a tender and soft swelling at the right sided parietal bone (Figure 2B), which was also positive for Ga[67] scintigraphy. This tumor was again resected. Both tumors were diagnosed as LCH. Currently at age 46, the patient has been followed up without receiving any systemic chemotherapy and in a state of ASAD.

Case 8

A 40-year-old male was found to have a mass at the left articular arch to the spinous process of C6, which was significantly hot (SUVmax; 6.6) with PET scan (Figure 3). The mass was biopsied, which was diagnosed to be LCH. The CT scan showed the lymphadenopathy at the bilateral axillary as well as inguinal area. Thus, an inguinal node was biopsied, which also showed LCH with complex karyotypes. Past history showed he had a severe atopic dermatitis since age of 20, treated with Protopic (tacrolimus hydrate) ointment. He was treated with systemic chemotherapy [VBL/methotrexate (MTX)/PSL/bisphosphonate]. The patient has currently been treated for active C6 lesion.
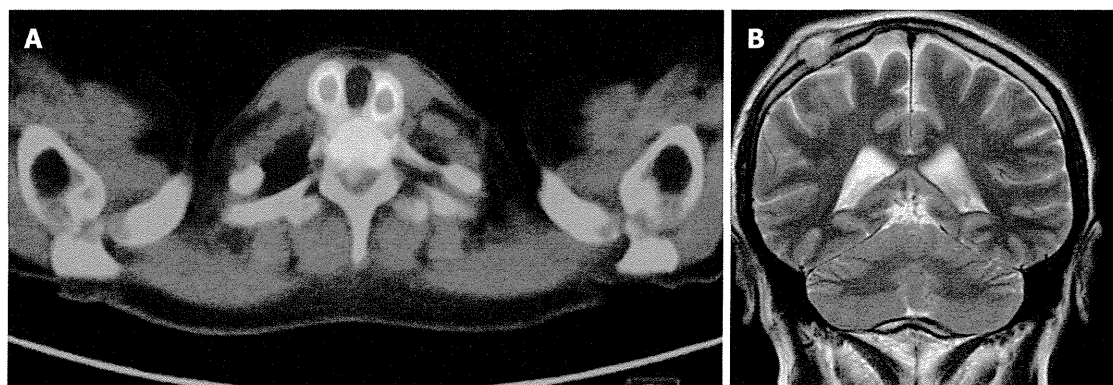
Figure 2 langerhans cell histiocytosis thyroid (A) and skull (B) lesions. A: Positron emission tomography scan shows hot spots (SUVmax = 7.0) at both lobes of thyroid; B: Magnetic resonance imaging (T2W2) shows a mass at the right parietal region.
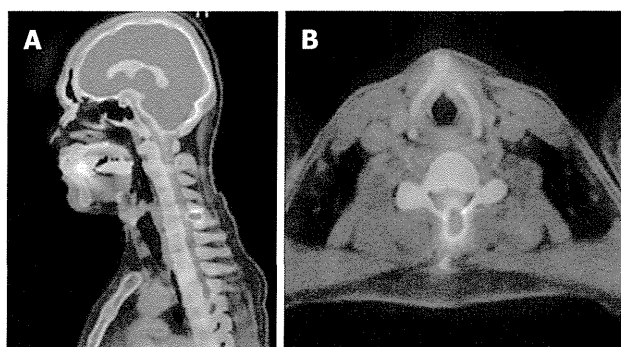
Figure 3 langerhans cell histiocytosis bone lesion at cervical vertebra 6. Positron emission tomography scan shows a hot spot (SUVmax = 6.6) at the spinous process of C6. A: Sagittal view; B: Axial view.

Case 9

A 27-year-old female, who had been treated for atopic dermatitis since childhood, was noted to have a swelling at the right orbit. MRI showed a mass lesion at the right temporal bone extended to the adjacent muscle, which consisted of heterogeneous components (Figure 4A and B). The mass was extensively removed by surgery and the diagnosis of LCH was made. PET scan did not reveal any other suspected lesions. Thus, she was put on observation alone. The patient has been followed up longer than two years without reactivation of the disease. No CDI has occurred and the patient has been in a state of ASAD.

Case 10

A 31-year-old male was first noted to have 1st thoracic spine lesion at age 25, which was biopsied and diagnosed as LCH. Two years later the systemic bone survey revealed a skull lesion, which was surgically removed. Two more years later, he had difficulty in opening mouth and was diagnosed to have a lesion at the mandible bone. Since then he was treated with PSL and bisphosphonate. Nevertheless, he complained of right sided lumbago two more years later due to the involvement of newly appeared iliac bone lesions. Currently the patient has had multiple bone lesions as well as CDI. He needed further systemic chemotherapy for active disease.

Case 11

A 53-year-old female first developed CDI at age of 41. Two years later, she was noted to have a right mandibular bone mass which was totally resected; however, diagnosis remained unknown. Three more years later she developed bone lesions at the frontal to left temporal skull, which caused a diffuse bone defect, including skull and facial bones (Figure 4C), when LCH was diagnosed. With systemic CT scan, she also was noted to have multiple osteolytic lesions at the skull, spine, scapula, rib and pelvis. She received LCH-A1 protocol[6], consisting of VBL and PSL for a year, which induced a new bone synthesis at the frontal bone. More recently, 12 years after the onset of initial symptoms, she has had newly-developed left mandibular osteolysis. She has currently been treated for active disease.

Case 12

A 36-year-old female was noted to have amenorrhea even after stopping milk feeding for her first-born baby. Administration of Gonadotropin-releasing hormone was successful in resuming a menstrual cycle and she gave birth of second child; however, soon after second childbirth she complained of symptoms compatible with CDI, when brain MRI showed a loss of bright spot at the pituitary posterior lobe; in addition, almost a year later, she was found to have a hypothalamic mass with a gadolinium (Gd)-enhanced MRI (Figure 5A). Biopsy of the mass confirmed the diagnosis of LCH. Since the probable compression of cerebrum due to a huge mass caused impaired consciousness, the patient received systemic chemotherapy, first with VBL followed by 2CDA.

Case 13

A 20-year-old girl first complained of polyuria/polydipsia and amenorrhea. Eight months later, she was detected a Gd-enhanced mass at the HPR by a brain MRI. An immediate open biopsy of the mass confirmed the diagnosis of LCH. Initially, irradiation (21 Gy) to the CNS markedly reduced the size of mass. Two years later, the patient was noted to have re-growth of hypothalamic mass, continued amenorrhea, poorly-controlled CDI and generalized cutaneous LCH, which was confirmed by
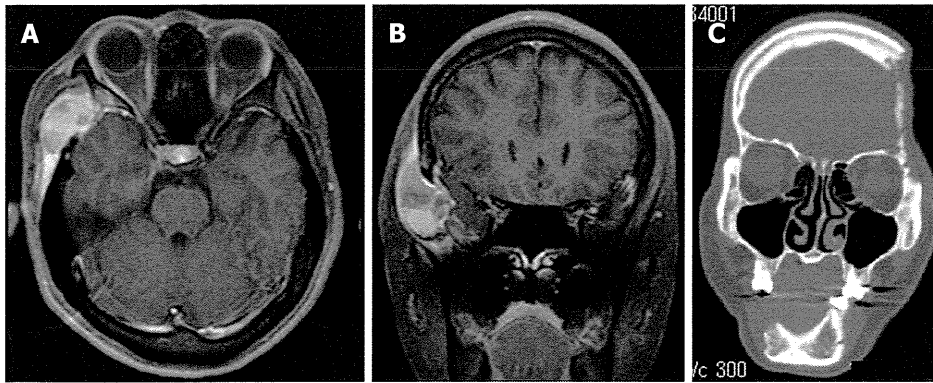
Figure 4 Langerhans cell histiocytosis skull mass (A, B) and lytic skull (C) lesion. A, B: Gadolinium-enhanced magnetic resonance imaging (T1W1) shows a mass with heterodensity at the right temporal area. axial view (A), coronal view (B); C: Computed tomography scan shows extensive lytic bones, at the left temporal bone and mandible. Defect of the right mandible is due to surgical resection.
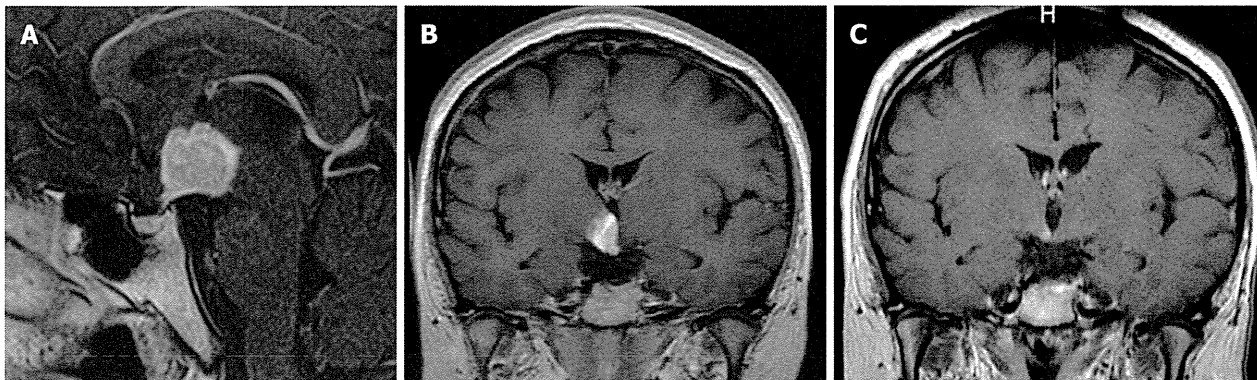
Figure 5 Langerhans cell histiocytosis mass at the hypothalamic area (A) and hypothalamic–pituitary area, comparison of pre and post chemotherapy (B, C). A: Gadolinium-enhanced magnetic resonance imaging (W1T1) shows a large mass at the hypothalamic area. Pituitary stalk is enlarged; B, C: Gadolinium-enhanced magnetic resonance imaging (T1W1) shows (B) a large mass before chemotherapy and (C) a residual mass post chemotherapy. The size of mass was significantly reduced after 2-deoxychloroadenosine treatment.

biopsy. Re-institution of systemic chemotherapy significantly (> 50%) reduced the size of hypothalamic mass. The patient has currently been in a state of ASAD.

Case 14

A 36-year-old female developed CDI in association with amenorrhea. However, the thickened pituitary stalk detected by MRI was put on under observation and not immediately treated. After progression of the thickened pituitary stalk into a significant Gd-enhanced mass at the HPR, a biopsy was performed to reveal typical LCH histology, when the patient had amenorrhea, fatty liver, reduced glucose tolerance. Systemic chemotherapy with 2CDA significantly (> 50%) reduced the mass size (Figure 5B and C). LCH lesions outside the CNS were not found. The patient remains markedly obese and diabetic, with residual active disease.

Case 15

A 38-year-old male was first diagnosed with primary hypothyroidism. Nineteen months later, he developed the symptoms of CDI, fatigue and disturbed consciousness along with disorientation and abnormal behaviors. A brain MRI revealed a Gd-enhanced mass at the HPR,

which biopsy did not confirm the diagnosis of LCH. Two years later, osteolytic bone lesions appeared on the right femur and left clavicle, when the LCH was eventually diagnosed by a bone biopsy. The patient received systemic chemotherapy with 2CDA, but the mass size was reduced minimally (< 50%), and he remained significantly obese and diabetic. Four years from the initial CDI symptom, the patient developed retropharyngeal B-cell lymphoma. He has had active diseases of LCH as well as lymphoma.

Case 16

A 46-year-old male first presented with decreased libido and erectile dysfunction seven years after total gastrectomy for gastric adenocarcinoma. Four years later, a Gd-enhanced mass at the HPR was detected. Until then, he had ignored his polydipsia/polyuria symptoms, thus the diagnosis of CDI was delayed. Biopsy of the CNS mass led to a diagnosis of LCH. A systemic MRI survey also revealed multiple spinal involvements. The patient also had loss of concentration and short term memory deficits suggesting mild neurodegenerative disease, which findings were confirmed with brain MRI examination. Eventually, the patients received systemic chemotherapy
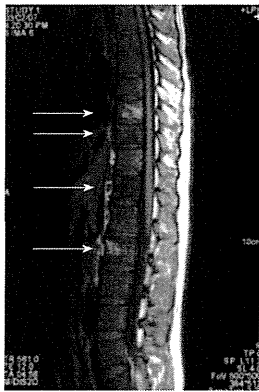
Figure 6 Langerhans cell histiocytosis spinal lesions. Non-enhanced magnetic resonance imaging (T1W1) shows high and low signals at multiple vertebral bodies (arrows).

with 2CDA, which markedly (> 50%) reduced the CNS mass size. However, currently, he has been treated for the regrowth of the CNS mass.

Case 17

A 23-year-old young adult was noted to have cerebellar ataxia and dysarthria. Past history revealed that at age of 16, he had been diagnosed as CDI; however, the exact cause was unidentified. At age 20, he was found to have polycystic lung disease with pneumothorax, followed by a mild ataxia. At age 23, he suffered a traffic accident when he was incidentally found to have a brain disease with a mass at the HPR as well as neurodegenerative disease on MRI performed at the emergency hospital. Eventually, LCH was diagnosed from the biopsy of lung tissues. He received monthly intravenous immunoglobulin therapy for neurodegenerative disease with dexamethasone[10]; however, the patient declined further treatment. Currently, he has remained with progressive neurological symptoms and with active lung disease.

Case 18

An 18-year-old man initially complained of low back pain and cervical mass. MRI revealed multiple spinal bone involvement (Figure 6). The initial diagnosis of LCH was made from the histology obtained by excisional iliac biopsy. A year later, he developed swelling of left cervical lymph nodes. CT scan of the chest also revealed a nodule in the right lung and the enlargement of left upper mediastinal lymph nodes. Histopathology of the biopsied cervical lymph node showed coexistence of two tumorous components; one was LCH and the other tissue of Hodgkin disease with Reed-Sternberg/Hodgkin cells being positive for CD30. The disease responded temporarily to irradiation (36 Gy) and systemic chemotherapy, but became refractory with relapses to the lungs and lymph nodes. Despite autologous followed by allogeneic HSCTs, he died of refractory Hodgkin disease at age of 23.

Summary of the cases

As summarized in Table 1, cases consisted of 3 SS-LCH

(all CNS disease) and 15 MS-LCH. Regarding the initial symptoms, 7 (2 males and 5 females) of the 18 patients had CDI and other endocrine symptoms with thickened pituitary stalk or a mass at the HPR. Additional 2 patients initiated the disease with CDI with no immediate diagnosis. In the remaining patients, the disease begun with single (n = 3) or multiple (n = 1) spinal bone lesion(s) in 4 patients (all males), with multiple bone lesions in 3 patients (1 male and 2 females), with localized skull/muscle lesion in one female patient and with ambiguous symptoms including hypothyroidism in one male patient. Thyroid mass was noted in 2 patients. In terms of treatment, 9 patients received systemic immuno-chemotherapy alone, of whom 3 with CNS disease and 1 with multiple bone lesions received 2CDA. Five patients had a combination of immuno-chemotherapy with surgical resection or radiotherapy, 2 had immunotherapy alone, 2 had surgical resection followed by observation alone to date. Three patients received HSCT after extensive chemotherapy. In terms of outcome, 15 patients are alive (9 with active disease; AWAD, 6 without active disease; ASAD) with a median follow-up of 66 mo (range 17-166 mo) and 2 died of disease; 1 from sepsis-induced DIC and the other from progression of Hodgkin disease. The remaining 1 patient is lost to follow-up. As late sequelae, CDI (n = 9), neurodegenerative disease (n = 2) and obesity/diabetes mellitus (n = 3) are noted.

DISCUSSION

Clinical features

To date, adult LCH cases have mostly been reported as case series[14-18]. Here, we add another case series describing the clinical features and discussing the issues specifically relevant to adult LCH. Adult patients may have LCH as a recurrence of childhood LCH as well as *de novo* LCH developing first in adult life. Here described is all the latter type of LCH. None had a history of LCH in childhood.

Two major clinical features of non-pulmonary LCH in adults

It is apparent that there are two major groups; one is a CNS mass with endocrine problems (9/18) and the other is recalcitrant bone lesions (7/18). Both types of disease are histologically non-malignant, but extensive disease causes various impairments leading to the decreased quality of life, and limiting to achieve normal daily life activity.

Endocrine problems

Adult patients are often noted first with endocrine problems such as CDI, amenorrhea, loss of libido and obesity[9]. Particularly, hypothalamic-pituitary disease is the most common CNS manifestation of LCH, which leads to CDI and anterior pituitary hormone deficiencies. CDI is diagnosed from the finding that MRI scan shows absence of the bright spot of the posterior pituitary on

−40−

Table 1 Summary of 18 cases of non-pulmonary adult langerhans cell histiocytosis

Cases	Age (yr)/sex	Initial symptoms/signs	Subsequent symptoms/ disease progression	Treatment			Outcome	Follow-up (mo)
				Surgical resection	Radiation	Immune-chemo Rx/HSCT		
1	27/F	CDI/endocrine	None	Y	Y	Y[4]	LTF	-
2	25/F	CDI/endocrine	Nasal/thyroid/skin masses			Y	DOD[1]	216
3	35/F	MBL	MBL			Y/Y	ASAD	132+
4	37/M	CDI	MBL/skin lesions			Y/Y	ASAD	128+
5	40/M	MBL	MBL		Y	Y	ASAD	133+
6	46/F	Thyroid mass/spine (Th4)	MBL/LNs	Y		Y	AWAD	27+
7	40/M	Spine (C3)	Parietal bone	Y			ASAD	72+
8	40/M	Spine (C6)	Inguinal LNs			Y	AWAD	17+
9	27/F	Temporal bone	None	Y			ASAD	26+
10	31/M	Spine (Th1)	MBL			Y[4]	AWAD	108+
11	53/F	CDI	MBL	Y		Y	AWAD	166+
12	36/F	Endocrine	HPR mass			Y[3]	AWAD	28+
13	20/F	CDI/endocrine	Skin		Y	Y	ASAD	156+
14	36/F	CDI/endocrine	None			Y[3]	AWAD	52+
15	38/M	Hypothyroid	CDI/endocrine			Y[3]	AWAD	48+
16	46/M	Endocrine	CDI/MBL/ND-CNS			Y[3]	AWAD	60+
17	23/M	CDI	Lungs/ND-CNS			Y[4]	AWAD	72+
18	18/M	Spine (multiple)	LNs/Lungs		Y	Y/Y	DOD[2]	72

[1]From disseminated intravascular coagulation; [2]From Hodgkin disease; [3]Systemic chemotherapy with 2-deoxychloroadenosine; [4]Steroid alone with or without bisphosphonate. CDI: Central diabetes insipidus; MBL: Multiple bone lesions; HPR: Hypothalamic pituitary region; LNs: Lymph nodes; ND-CNS: Neurodegenerative central nervous system disease; Y: Yes; LTF: Lost to follow-up; ASAD: Alive without active disease; AWAD: Alive with active disease; DOD: Died of disease.

the T1-weighted sequences[9,19]; however, it is common that patients are taken care and followed up about these problems at the Endocrinology Unit until when Gd-enhanced MRI reveals a thickened pituitary stalk and/or a hypothalamic mass. Generally, it takes a year or longer for the mass to be biopsied and correct diagnosis be confirmed. Even when the diagnosis is confirmed, there are occasions that it takes time for the patient to be referred to hemato-oncologists for chemotherapy. Whenever the diagnosis and the introduction of treatment are delayed, the patient may develop not only endocrine problems but also cognitive impairment such as memory deficits as well as consciousness disturbances, as shown in our cases (Cases 12, 16, 17).

LCH in association with childbirth
The development of LCH in association with childbirth has not been well recognized. Regarding LCH occurring during pregnancy, only a few sporadic cases have been described previously[20,21]; however, no information is available how childbirth influenced on the development of LCH. In our series, the correlation between pregnancy/childbirth and LCH in adult female patients was noted in 4 cases (Cases 1-3, 12). Sex hormones are believed to participate in immune responses, as estrogens have been found to serve as enhancers in humoral immunity while androgens/progesterone appears to act as natural immune-suppressors[22]. For examples, postpartum thyroiditis/diabetes mellitus is speculated to be a consequence of the immunological flare that occurs after the lifting of the pregnancy-related immune suppression[23,24]. Moreover, pregnancy and the post-partum period are associated with

increased breast cancer aggressiveness[25]. Thus, the hormonal imbalance in the postpartum period may trigger the development of LCH. Detailed examination of pregnancy and childbirth history in female LCH patients may clarify whether the associated hormonal changes influence the pathogenesis and the development of LCH.

LCH in association with various diseases/events
Two patients (Cases 16, 17) were noted to have cognitive disturbance due to LCH-related neurodegenerative CNS disease[10]. Additionally, two patients (Cases 15, 18) developed malignant lymphoma; one with concurrent LCH and Hodgkin disease and the other developed B-cell lymphoma after systemic chemotherapy for LCH. The association of LCH and other malignant lymphoid neoplasms has been well recognized[26-28]. In this series two patients (Cases 8, 9) with severe atopic dermatitis were found to develop LCH. This is an interesting topic considering the antigen-stimulation in the skin. It is also cautioned that recalcitrant or clinically atypical skin eruptions must be differentiated from LCH and other rare disorders[29] but no data is available that incidence of LCH is higher in patients with severe atopic dermatitis. Four patients (Cases 3, 5, 7, 8) were diagnosed to have LCH from spinal bone lesions. Particularly, of whom two had single spine (C3 or C6) involvement, not in the spinal body but in the arch. Spinal lesion should be searched for any adult who complained of cervical pain[30]. Intriguingly, discovery of LCH was triggered by road traffic accident in 2 patients (Cases 8, 17), although such reports are rarely found[31]. In Case 8, LCH lesion at the cervical spine was identified at the emergency hospital. In Case 17, traffic accident

incidentally led to the diagnosis of CNS- and pulmonary-LCH in the patient.

Importance of CT/MR/PET imaging for the diagnosis

To determine the precise biopsy/excision site of LCH, CT/MRI findings are inevitable. Particularly, bone scintigraphy for multiple bone lesions and Gd-enhanced MRI for CNS lesions are essential for the diagnosis of LCH[9,19]. However, more recently, ^{18}F-FDG PET is recommended. In one large study it was concluded that whole body FDG-PET scans can detect LCH activity and is useful to evaluate early response to therapy with greater accuracy than other imaging modalities (MRI, CT, plain films) in patients with LCH lesions in the bones and soft tissues[32]. Also, it is a useful tool for the monitoring of CNS disease activity in LCH[33,34]. It is said that ^{18}F-FDG PET might be useful to detect an early neurodegenerative lesions before MRI abnormalities appear, where bilateral hypometabolism is shown in the cerebellum and the basal ganglia (caudate nuclei) areas[34].

Therapeutic measures for adult LCH

In this case series, four patients received surgical resection of LCH mass without immuno-chemotherapy. Four patients received irradiation to the CNS-mass (n = 2), bone (n = 1) and lungs (n = 1), in association with immuno-chemotherapy. In the majority, systemic immuno-chemotherapy was given, mostly with a conventional combination of VBL/PSL or JCSL-96 protocol including VCR/cytosine arabinoside (AraC)/PSL[13] for induction. In 3 cases with CNS-LCH, 2CDA was employed. Previously proposed A1 protocol for adult LCH[6] was used only in one case in this series. With these measures, 6 ASAD cases were obtained, but necessity for further improvement of treatment for adult LCH seems apparent. As future trials, we have to scrutinize how efficiently we can employ AraC, 2CDA, clofarabine, and other novel agents for adult LCH patients. In the past, treatment reports on adult LCH cases were very limited[35,36]. In particular, the usefulness of intravenous 2CDA for CNS-LCH as well as for systemic MS-LCH was described in adult patients[37-40]. Windebank et al[41] also reported the usefulness of subcutaneous 2CDA treatment (5 mg/m^2 × 5 d, sc, q4 wk, for up to 6 cycles) in LCH. Effectiveness of the combination of 2CDA/AraC was described for extremely refractory cases[42]. More recently, effectiveness of clofarabine (25 mg/m^2 × 5 d, iv, q4 wk) has also been reported[43,44]. Particularly, Simko et al[44] demonstrated usefulness of clofarabine for multifocal skull lesions. On the other hand, Morimoto et al[11] reported the usefulness of Special C regimen of JLSG for treating adult LCH patients on ambulatory basis. Intriguingly, for the treatment of multiple bone LCH lesions in adults, Cantu et al[45] reported that AraC alone is an effective and minimally toxic, while VBL/PSL results in poor overall responses with excessive toxicity. Considering the fact that about 50% of LCH possess BRAF V600E mutation, molecular targetting treatment with vemurafenib has been proposed

Protocol	Drugs	Ref.
A1 protocol	VBL/PSL	[6]
JLSG-96	VCR/AraC/MTX/6MP/PSL	[13]
Cladribine-based	2CDA/PSL, 2CDA/AraC	[37-41]
Clofarabine-based	Clofarabine	[43,44]
JLSG-special C	VBL/MTX/6MP/PSL	[11]
Others	AraC alone	[45]
Molecular targetting	Vemurafenib	[46]
Bone therapy	Zoledronic acid	[47]

Table 2 Therapeutic options in the treatment of adult langerhans cell histiocytosis

VBL: Vinblastine; PSL: Prednisolone; MTX: Methotrexate; 6MP: 6-mercatopurine hydrate; 2CDA: 2-deoxychloroadenosine.

more recently[46]. As bone therapy regimen, Zoledronic acid as bisphosphonate is available, although its effectiveness on LCH bone lesions is still elusive[47]. Allogeneic HSCT for adult LCH is not within a scope of this article, although a few reports on pediatric LCH cases have been described[48,49]. As well recognized, in the recipients of allogeneic HSCT, care must be taken for the transplant related adverse events. In Table 2, a list of candidate systemic immuno-chemotherapy regimens is summarized, which we think is useful in choosing regimens for adult LCH patients. In practice, for an adult case of LCH with persistent minimal disease and systemic involvement, we prefer once a month or twice a month treatment, like Special C regimen of JLSG[11]. However, with these regimens, some adult patients may still show VBL neurotoxicity, MTX hepatotoxicity, or neutropenia due to mercatopurine hydrate (6MP); such events make it difficult to achieve the entire regimens as planned. Although we recognize that 2CDA is highly effective and could be useful in adult LCH, it is often difficult persuading the patients to stay in the hospital for the 5-d continuous treatment. If subcutaneous 2CDA is available at the outpatient care, this agent could be more employed in the treatment of adult LCH. In any case, it is important to make a most appropriate treatment plan for each patient individually. In summary, for adult patients with two major types of LCH, i.e., recalcitrant multiple bone lesions and/or a mass at the HPR, early introduction of systemic immuno-chemotherapy using conventional regimens including AraC or alternative 2CDA or clofarabine regimens is recommended to overcome the disease-related impairment of qualify of life.

ACKNOWLEDGEMENTS

REFERENCES

1   Egeler RM, Annels NE, Hogendoorn PC. Langerhans cell histiocytosis: a pathologic combination of oncogenesis and immune dysregulation. *Pediatr Blood Cancer* 2004; 42: 401-403 [PMID: 15049009 DOI: 10.1002/pbc.10464]

2   Abla O, Egeler RM, Weitzman S. Langerhans cell histiocytosis: Current concepts and treatments. *Cancer Treat Rev* 2010; 36: 354-359 [PMID: 20188480 DOI: 10.1016/j.ctrv.2010.02.012]

3   Badalian-Very G, Vergilio JA, Degar BA, Rodriguez-Galindo C, Rollins BJ. Recent advances in the understanding of Langerhans cell histiocytosis. *Br J Haematol* 2012; 156: 163-172 [PMID: 22017623 DOI: 10.1111/j.1365-2141.2011.08915.x]

4   Imashuku S, Ikushima S, Hibi S. Langerhans cell histiocytosis in adults in Japan. *Med Pediatr Oncol* 1998; 31: 47

5   Aricò M, Girschikofsky M, Généreau T, Klersy C, McClain K, Grois N, Emile JF, Lukina E, De Juli E, Danesino C. Langerhans cell histiocytosis in adults. Report from the International Registry of the Histiocyte Society. *Eur J Cancer* 2003; 39: 2341-2348 [PMID: 14556926]

6   Arico M, de Juli E, Genereau T, Saven A. Special aspects of Langerhans cell histiocytosis in adult. In: Weitzman S, Egeler RM, editors. Histiocytic Disorders of Children and Adults. Cambridge: Cambridge University Press, 2005: 174-186

7   Vassallo R, Ryu JH. Smoking-related interstitial lung diseases. *Clin Chest Med* 2012; 33: 165-178 [PMID: 22365253 DOI: 10.1016/j.ccm.2004.04.005]

8   Sundar KM, Gosselin MV, Chung HL, Cahill BC. Pulmonary Langerhans cell histiocytosis: emerging concepts in pathobiology, radiology, and clinical evolution of disease. *Chest* 2003; 123: 1673-1683 [PMID: 12740289 DOI: 10.1378/chest.123.5.1673]

9   Imashuku S, Kudo N, Kaneda S, Kuroda H, Shiwa T, Hiraiwa T, Inagaki A, Morimoto A. Treatment of patients with hypothalamic-pituitary lesions as adult-onset Langerhans cell histiocytosis. *Int J Hematol* 2011; 94: 556-560 [PMID: 22015494 DOI: 10.1007/s12185-011-0955-z]

10   Imashuku S, Shioda Y, Kobayashi R, Hosoi G, Fujino H, Seto S, Wakita H, Oka A, Okazaki N, Fujita N, Minato T, Koike K, Tsunematsu Y, Morimoto A. Neurodegenerative central nervous system disease as late sequelae of Langerhans cell histiocytosis. Report from the Japan LCH Study Group. *Haematologica* 2008; 93: 615-618 [PMID: 18287136 DOI: 10.3324/haematol.11827]

11   Morimoto A, Shimazaki C, Takahashi S, Yoshikawa K, Nishimura R, Wakita H, Kobayashi Y, Kanegane H, Tojo A, Imamura T, Imashuku S. Therapeutic outcome of multifocal Langerhans cell histiocytosis in adults treated with the Special C regimen formulated by the Japan LCH Study Group. *Int J Hematol* 2013; 97: 103-108 [PMID: 23243004 DOI: 10.1007/s12185-012-1245-0]

12   Hirasaki S, Murakami K, Mizushima T, Koide N. Multifocal Langerhans cell histiocytosis in an adult. *Intern Med* 2012; 51: 119-120 [PMID: 22214636 DOI: 10.2169/internalmedicine.51.6630]

13   Morimoto A, Ikushima S, Kinugawa N, Ishii E, Kohdera U, Sako M, Fujimoto J, Bessho F, Horibe K, Tsunematsu Y, Imashuku S. Improved outcome in the treatment of pediatric multifocal Langerhans cell histiocytosis: Results from the Japan Langerhans Cell Histiocytosis Study Group-96 protocol study. *Cancer* 2006; 107: 613-619 [PMID: 16804933 DOI: 10.1002/cncr.21985]

14   Kilpatrick SE, Wenger DE, Gilchrist GS, Shives TC, Wollan PC, Unni KK. Langerhans' cell histiocytosis (histiocytosis X) of bone. A clinicopathologic analysis of 263 pediatric and adult cases. *Cancer* 1995; 76: 2471-2484 [PMID: 8625073]

15   Malpas JS, Norton AJ. Langerhans cell histiocytosis in the adult. *Med Pediatr Oncol* 1996; 27: 540-546 [PMID: 8888814]

16   Baumgartner I, von Hochstetter A, Baumert B, Luetolf U, Follath F. Langerhans'-cell histiocytosis in adults. *Med Pediatr Oncol* 1997; 28: 9-14 [PMID: 8950330]

17   Götz G, Fichter J. Langerhans'-cell histiocytosis in 58 adults. *Eur J Med Res* 2004; 9: 510-514 [PMID: 15649860]

18   Giona F, Caruso R, Testi AM, Moleti ML, Malagnino F, Martelli M, Ruco L, Giannetti GP, Annibali S, Mandelli F. Langerhans' cell histiocytosis in adults: a clinical and therapeutic analysis of 11 patients from a single institution. *Cancer* 1997; 80: 1786-1791 [PMID: 9351548]

19   Kaltsas GA, Powles TB, Evanson J, Plowman PN, Drinkwater JE, Jenkins PJ, Monson JP, Besser GM, Grossman AB. Hypothalamo-pituitary abnormalities in adult patients with langerhans cell histiocytosis: clinical, endocrinological, and radiological features and response to treatment. *J Clin Endocrinol Metab* 2000; 85: 1370-1376 [PMID: 10770168 DOI: 10.1210/jc.85.4.1370]

20   DiMaggio LA, Lippes HA, Lee RV. Histiocytosis X and pregnancy. *Obstet Gynecol* 1995; 85: 806-809 [PMID: 7724119 DOI: 10.1016/0029-7844(94)00404-2]

21   Gutiérrez Cruz O, Careaga Benítez R. [Diabetes insipidus and pregnancy]. *Ginecol Obstet Mex* 2007; 75: 224-229 [PMID: 17849803]

22   Cutolo M, Sulli A, Capellino S, Villaggio B, Montagna P, Seriolo B, Straub RH. Sex hormones influence on the immune system: basic and clinical aspects in autoimmunity. *Lupus* 2004; 13: 635-638 [PMID: 15485092 DOI: 10.1191/0961203304lu1094oa]

23   Terry AJ, Hague WM. Postpartum thyroiditis. *Semin Perinatol* 1998; 22: 497-502 [PMID: 9880119 DOI: 10.1016/S0146-0005(98)80029-3]

24   Füchtenbusch M, Ferber K, Standl E, Ziegler AG. Prediction of type 1 diabetes postpartum in patients with gestational diabetes mellitus by combined islet cell autoantibody screening: a prospective multicenter study. *Diabetes* 1997; 46: 1459-1467 [PMID: 9287047]

25   Mathelin C, Annane K, Treisser A, Chenard MP, Tomasetto C, Bellocq JP, Rio MC. Pregnancy and post-partum breast cancer: a prospective study. *Anticancer Res* 2008; 28: 2447-2452 [PMID: 18751433]

26   Adu-Poku K, Thomas DW, Khan MK, Holgate CS, Smith ME. Langerhans cell histiocytosis in sequential discordant lymphoma. *J Clin Pathol* 2005; 58: 104-106 [PMID: 15623497 DOI: 10.1136/jcp.2003.015537]

27   Shin MS, Buchalter SE, Ho KJ. Langerhans' cell histiocytosis associated with Hodgkin's disease: a case report. *J Natl Med Assoc* 1994; 86: 65-69 [PMID: 8151725]

28   Naumann R, Beuthien-Baumann B, Fischer R, Kittner T, Bredow J, Kropp J, Ockert D, Ehninger G. Simultaneous occurrence of Hodgkin's lymphoma and eosinophilic granuloma: a potential pitfall in positron emission tomography imaging. *Clin Lymphoma* 2002; 3: 121-124 [PMID: 12435286 DOI: 10.3816/CLM.2002.n.019]

29   Sires UI, Mallory SB. Diaper dermatitis. How to treat and prevent. *Postgrad Med* 1995; 98: 79-84, 86 [PMID: 7501582]

30   Simanski C, Bouillon B, Brockmann M, Tiling T. The Langerhans' cell histiocytosis (eosinophilic granuloma) of the cervical spine: a rare diagnosis of cervical pain. *Magn Reson Imaging* 2004; 22: 589-594 [PMID: 15120180 DOI: 10.1016/j.mri.2004.01.006]

31   Lee YS, Kwon JT, Park YS. Eosinophilic granuloma presenting as an epidural hematoma and cyst. *J Korean Neurosurg Soc* 2008; 43: 304-306 [PMID: 19096637 DOI: 10.3340/jkns.2008.43.6.304]

32   Phillips M, Allen C, Gerson P, McClain K. Comparison of

FDG-PET scans to conventional radiography and bone scans in management of Langerhans cell histiocytosis. *Pediatr Blood Cancer* 2009; **52**: 97-101 [PMID: 18951435 DOI: 10.1002/pbc.21782]

33   **Büchler T**, Cervinek L, Belohlavek O, Kantorova I, Mechl M, Nebesky T, Vorlicek J, Adam Z. Langerhans cell histiocytosis with central nervous system involvement: follow-up by FDG-PET during treatment with cladribine. *Pediatr Blood Cancer* 2005; **44**: 286-288 [PMID: 15481071 DOI: 10.1002/pbc.20175]

34   **Ribeiro MJ**, Idbaih A, Thomas C, Remy P, Martin-Duverneuil N, Samson Y, Donadieu J, Hoang-Xuan K. 18F-FDG PET in neurodegenerative Langerhans cell histiocytosis : results and potential interest for an early diagnosis of the disease. *J Neurol* 2008; **255**: 575-580 [PMID: 18227990 DOI: 10.1007/s00415-008-0751-8]

35   **McClain K**, Allen C, Ebrahim S. Review of histiocytosis treatment and neurotoxicity in adult patients. *Pediatr Blood Cancer* 2009; **53**: 696

36   **Derenzini E**, Fina MP, Stefoni V, Pellegrini C, Venturini F, Broccoli A, Gandolfi L, Pileri S, Fanti S, Lopci E, Castellucci P, Agostinelli C, Baccarani M, Zinzani PL. MACOP-B regimen in the treatment of adult Langerhans cell histiocytosis: experience on seven patients. *Ann Oncol* 2010; **21**: 1173-1178 [PMID: 19861578 DOI: 10.1093/annonc/mdp455]

37   **Saven A**, Burian C. Cladribine activity in adult langerhans-cell histiocytosis. *Blood* 1999; **93**: 4125-4130 [PMID: 10361109]

38   **Adam Z**, Szturz P, Duraš J, Pour L, Krejčí M, Rehák Z, Koukalová R, Navrátil M, Hájek R, Král Z, Mayer J. [Treatment of Langerhans cells histiocytosis by cladribin reached long-term complete remission in 9 out of 10 adult patients]. *Klin Onkol* 2012; **25**: 255-261 [PMID: 22920165]

39   **Weitzman S**, Braier J, Donadieu J, Egeler RM, Grois N, Ladisch S, Pötschger U, Webb D, Whitlock J, Arceci RJ. 2'-Chlorodeoxyadenosine (2-CdA) as salvage therapy for Langerhans cell histiocytosis (LCH). results of the LCH-S-98 protocol of the Histiocyte Society. *Pediatr Blood Cancer* 2009; **53**: 1271-1276 [PMID: 19731321 DOI: 10.1002/pbc.22229]

40   **Schini M**, Makras P, Kanakis G, Voulgarelis M, Kaltsas G. Cladribine therapy in adults with advanced Langerhans cell histiocytosis. *Leuk Lymphoma* 2012; Epub ahead of print [PMID: 23101752 DOI: 10.3109/10428194.2012.744454]

41   **Windebank K**, Bigley V, Zammit I, Haniffa M, Nanduri V, Collin M. Treatment of adult LCH with subcutaneous cladribine. 28th Annual meeting of the Histiocyte Society; London, United Kingdom. 2012: 38

42   **Bernard F**, Thomas C, Bertrand Y, Munzer M, Landman Parker J, Ouache M, Colin VM, Perel Y, Chastagner P, Vermylen C, Donadieu J. Multi-centre pilot study of 2-chlorodeoxyadenosine and cytosine arabinoside combined chemotherapy in refractory Langerhans cell histiocytosis with haematological dysfunction. *Eur J Cancer* 2005; **41**: 2682-2689 [PMID: 16291085 DOI: 10.1016/j.ejca.2005.02.007]

43   **Rodriguez-Galindo C**, Jeng M, Khuu P, McCarville MB, Jeha S. Clofarabine in refractory Langerhans cell histiocytosis. *Pediatr Blood Cancer* 2008; **51**: 703-706 [PMID: 18623218 DOI: 10.1002/pbc.21668]

44   **Simko S**, Allen C, Hicks J, McClain K. Clofarabine as salvage therapy in histiocytic disorders. 28th Annual meeting of the Histiocyte Society; London, United Kingdom. 2012: 31

45   **Cantu MA**, Lupo PJ, Bilgi M, Hicks MJ, Allen CE, McClain KL. Optimal therapy for adults with Langerhans cell histiocytosis bone lesions. *PLoS One* 2012; **7**: e43257 [PMID: 22916233 DOI: 10.1371/journal.pone.0043257]

46   **Haroche J**, Cohen-Aubart F, Emile JF, Arnaud L, Maksud P, Charlotte F, Cluzel P, Drier A, Hervier B, Benameur N, Besnard S, Donadieu J, Amoura Z. Dramatic efficacy of vemurafenib in both multisystemic and refractory Erdheim-Chester disease and Langerhans cell histiocytosis harboring the BRAF V600E mutation. *Blood* 2013; **121**: 1495-1500 [PMID: 23258922 DOI: 10.1182/blood-2012-07-446286]

47   **Montella L**, Merola C, Merola G, Petillo L, Palmieri G. Zoledronic acid in treatment of bone lesions by Langerhans cell histiocytosis. *J Bone Miner Metab* 2009; **27**: 110-113 [PMID: 19018458 DOI: 10.1007/s00774-008-0001-2]

48   **Steiner M**, Matthes-Martin S, Attarbaschi A, Minkov M, Grois N, Unger E, Holter W, Vormoor J, Wawer A, Ouachee M, Woessmann W, Gadner H. Improved outcome of treatment-resistant high-risk Langerhans cell histiocytosis after allogeneic stem cell transplantation with reduced-intensity conditioning. *Bone Marrow Transplant* 2005; **36**: 215-225 [PMID: 15937510 DOI: 10.1038/sj.bmt.1705015]

49   **Kudo K**, Ohga S, Morimoto A, Ishida Y, Suzuki N, Hasegawa D, Nagatoshi Y, Kato S, Ishii E. Improved outcome of refractory Langerhans cell histiocytosis in children with hematopoietic stem cell transplantation in Japan. *Bone Marrow Transplant* 2010; **45**: 901-906 [PMID: 19767778 DOI: 10.1038/bmt.2009.245]

ELSEVIER

Original contribution

Merkel cell polyomavirus DNA sequences in peripheral blood and tissues from patients with Langerhans cell histiocytosis[☆],[☆☆]

Ichiro Murakami MD, PhD[a],[*], Michiko Matsushita MT, MA[b], Takeshi Iwasaki MD[a], Satoshi Kuwamoto MD, PhD[a], Masako Kato MD, PhD[a], Yasushi Horie MD, PhD[c], Kazuhiko Hayashi MD, PhD[a], Toshihiko Imamura MD, PhD[d], Akira Morimoto MD, PhD[e], Shinsaku Imashuku MD, PhD[f], Jean Gogusev MD, PhD[g], Francis Jaubert MD, PhD[h], Katsuyoshi Takata MD, PhD[i], Takashi Oka PhD, DMSc[i], Tadashi Yoshino MD, PhD[i]

[a]Division of Molecular Pathology, Faculty of Medicine, Tottori University, Yonago 683–8503, Japan
[b]Department of Pathobiological Science and Technology, School of Health Science, Faculty of Medicine, Tottori University, Yonago 683–8503, Japan
[c]Department of Pathology, Tottori University Hospital, Yonago 683–8503, Japan
[d]Department of Pediatrics, Kyoto Prefectural University of Medicine, Kyoto 602–8566, Japan
[e]Department of Pediatrics, Jichi Medical University School of Medicine, Shimotsuke 329–0498, Japan
[f]Division of Pediatrics and Hematology, Takasago-seibu Hospital, Takasago 676–0812, Japan
[g]Inserm U507 and U1016, Institut Cochin, 75014 Paris, France
[h]University of Paris Descartes (Paris V), 75006 Paris, France
[i]Department of Pathology, Okayama University Graduate School of Medicine, Dentistry and Pharmaceutical Sciences, Okayama 700–8530, Japan

Summary Langerhans cell histiocytosis (LCH) is a group of granulomatous disorders in which abnormal Langerhans cells proliferate as either a localized lesion in a single bone or disseminated disease involving two or more organs or systems. Because the different LCH forms exhibit significantly elevated levels of inflammatory molecules, including pro-inflammatory cytokines and tissue-degrading enzymes, we investigated for a possible viral trigger in LCH pathogenesis. We looked for Merkel cell polyomavirus (MCPyV) in peripheral blood cells and tissues using quantitative real-time PCR and immunohistochemistry staining with anti-MCPyV large T-antigen antibody. Our findings revealed elevated amounts of MCPyV DNA in the peripheral blood cells of 2 of 3 patients affected by LCH with high-risk organ involvement (RO+) and absence of MCPyV DNA in the blood cells in all 12 LCH-RO− patients ($P = .029$). With lower viral loads (0.002-0.033 copies/cell), an elevated number of MCPyV DNA sequences was detected in 12 LCH tissues in comparison with control tissues obtained from

---

patients with reactive lymphoid hyperplasia (0/5; $P = .0007$), skin diseases not related to LCH in children younger than 2 years (0/11; $P = .0007$), or dermatopathic lymphadenopathy (5/20; $P = .0002$). The data, including frequent but lower viral loads and low large-T antigen expression rate (2/13 LCH tissues), suggest that development of LCH as a reactive rather than a neoplastic process may be related to MCPyV infection.

1. Introduction

Langerhans cell histiocytosis (LCH) is a neoplastic lesion characterized by uncontrolled clonal proliferation of Langerhans cells (LCs) in a tissue environment containing other lymphoid cells [1–3]. The disease differs widely in clinical presentation, from a localized lesion as a single-system (SS-LCH) disease to a severe disseminated multisystem form (MS-LCH) [4]. The latter form is frequent in children younger than 2 years, whereas SS-LCH is more common in children older than 2 years [5].

The liver, spleen, and bone marrow are considered high-risk organs for LCH, whereas skin, bone, lymph nodes, gastrointestinal tissue, pituitary gland, and central nervous system are considered low-risk organs [4]. Therefore, LCH is classified clinically as either affecting at least one high-risk organ (RO+) or involving only organs without high risk (LCH-RO−) [4]. Although most patients with LCH-RO+ develop MS-LCH, in some patients having only one high-risk organ involved, the clinical course is milder, with symptoms similar to those observed in SS-LCH [6,7].

Although numerous studies have attempted to classify the LCH subtypes anatomically, no clear-cut consensus has yet been reached. For example, mutations in the proto-oncogene *BRAF* were found in 57% of a series of 61 cases, but there was no significant relation between the mutations and the clinical course of the disease [3]. An interleukin (IL)-17A autocrine LCH model of the severity of the disease was proposed [8], yet conflicting data remain, creating what often is described as the IL-17A controversy [9,10]. More recently, our group proposed an IL-17A endocrine model, showing a specific pattern of expression of the IL-17A receptor (IL-17RA) in relation to LCH subtype [11]. In fact, the IL-17A/IL-17RA autocrine/endocrine loop appears important in host defense, in that IL-17A boosts the pro-inflammatory reaction against viral aggression [12,13]. In the same context, we previously reported higher expression of phosphatase SHP-1 (also known as Tyrosine-protein phosphatase non-receptor type 6) [14], which by itself might promote Toll-like receptor–activated production of antiviral molecules such as interferon type I in abnormal LCH cells [15].

The LCH subtypes are associated with the release of inflammatory molecules such as pro-inflammatory cytokines and tissue-degrading enzymes [8,11,14,16,17] that are produced by LCs in contact with pathogens [18]. The most characteristic lesions observed in patients with LCH are skin maculopapular excrescences that imply involvement of an unknown dermotropic virus [4]. One such agent inducing LCH proliferation might be the common dermotropic Merkel cell polyomavirus (MCPyV) [19–21], the major pathogenic agent of Merkel cell carcinoma (MCC) of the skin [22,23]. Histologically, LCs are located above the middle of the prickle cell layer of the epidermis, whereas the Merkel cells are mostly sited in the basal layer of the epidermis. It was previously proposed that LCs capture external pathogens by elongation of dendrites beyond the tight junction barrier and function as antigen-presenting cells [24]. External pathogens might be recognized primarily by LCs or by a precursor LC present in the skin and not by the Merkel cells, as presently alleged.

In this report, elevated numbers of MCPyV DNA sequences were detected in the blood in two of three patients clinically classified as LCH-RO+. Altogether, the findings could be an important additional argument supporting the view that LCs behave as candidate sanctuary cells for asymptomatic MCPyV despite active antibody synthesis and that this pathogenic agent is involved in the development of LCH.

2. Patients and methods

2.1. Patients, peripheral blood, and LCH tissue samples

This study was approved by the Institutional Review Board of Okayama University Graduate School of Medicine, Dentistry, and Pharmaceutical Sciences, Okayama, Japan, and the Faculty of Medicine, Tottori University, Yonago, Japan.

Peripheral blood samples were obtained from 15 patients affected by LCH (6 SS-LCH, 9 MS-LCH; 3 LCH-RO+, 12 LCH-RO−). A total of 13 tissue samples from patients with LCH (7 SS-LCH, 6 MS-LCH; 1 LCH-RO+, 12 LCH-RO−) also were analyzed. As controls, 5 tissue samples from patients with reactive lymphoid hyperplasia (RLH), 11 from patients with skin diseases not related to LCH, and 20 from patients with dermatopathic lymphadenopathy (DLA) characterized by localized paracortical proliferation of epidermal LCs in the lymph nodes were analyzed. All tissues were prepared as formalin-fixed, paraffin-embedded (FFPE) samples.

Some of the LCH blood and tissue samples were obtained from patients included in the Japan LCH Study Group Registry between 2002 and 2009. Other samples were harvested from

patients at Okayama University Hospital or Tottori University Hospital between 2002 and 2011. The histopathologic diagnosis was established by conventional staining of histologic sections supplemented by immunohistochemical profiling using anti-CD1a and anti-S100 antibodies [25]. Tissue samples were fixed in 10% neutral-buffered formalin and embedded in paraffin. For immunohistochemistry (IHC) analysis, the sections were deparaffinized in xylene and rehydrated in a graded ethanol series. Anti-CD1a antibody (monoclonal mouse antihuman [IgG1, κ], O10; DAKO Japan, Kyoto, Japan) was used at a 1:100 dilution and anti-S100 antibody (polyclonal rabbit, Z0311; DAKO Japan) was used at a 1:1000 dilution. Endogenous peroxidase activity was blocked by hydrogen peroxide. For CD1a immunostaining, antigen retrieval was performed by heating the slides in 0.01 M citrate-buffered solution, pH 6.0, in a pressure cooker at 98°C for 15 minutes. The slides were then incubated for 1 hour in 5% skim milk and for 3 hours at 37°C with the primary antibodies against CD1a or S100. Samples were then incubated with secondary antibodies for 1 hour at room temperature and stained using the DAKO EnVision+ system (DAKO Japan) and 3,3'-diaminobenzidine as a chromogen followed by hematoxylin as a counterstain. Lymph nodes or skin samples were used as controls throughout.

2.2. DNA extraction

DNA was extracted from peripheral blood mononuclear cells (PBMCs) of patients with LCH and from LCH, RLH, non-LCH dermal diseases and DLA tissues. Extraction of DNA from PBMCs was performed using the proteinase K and phenol/chloroform/isoamyl alcohol (25:24:1 v/v/v) procedure. For tissue samples, DNA was extracted from the different paraffin blocks using the QIAamp DNA FFPE Tissue Kit and Mini Kit following the manufacturer's protocols (QIAGEN GmbH, Hilden, Germany).

2.3. Laser capture microdissection and DNA extraction

Laser capture microdissection was performed using an LMD7000 microscope (Leica Microsystems GmbH, Wetzler, Germany). The LCH or DLA lesions (FFPE tissue) were previously stained by immunolabeling with anti-S100 antibodies. Stained uncovered slides were air dried. Using conventional staining and CD1a immunostaining as references, approximately 1000 positive and negative LCH cells were collected by microdissection into 200-μL low-binding plastic tubes. The DNA was extracted using a QIAamp DNA Micro Kit (QIAGEN GmbH).

2.4. Multiplex Q-PCR for MCPyV detection

The quantitative real-time PCR (Q-PCR) was performed in a 10-μl reaction mix containing TaqMan Copy Number

Reference Assay RNaseP (Applied Biosystems, Foster City, CA) as the internal control. To determine the ratio of MCPyV DNA to MCPyV DNA from the reference MCC (MCC = 1.0) for each LCH case, Q-PCR was performed using an ABI PRISM 7900HT Sequence Detection System (Applied Biosystems). A total of 2 μL (~30 ng) of each DNA sample was amplified with 5 μL of EXPRESS qPCR Supermix with Premixed ROX (Invitrogen, Carlsbad, CA), 240 nmol/L of fluorescein-labeled locked nucleic acid hydrolysis probe 22 (5'-TGGTGGAG-3') from a Universal Probe Library (Roche Diagnostics, Basel, Switzerland), and 0.9 μmol/L of a primer in a final volume of 10 μL. A primer pair targeting the position 859–934 on MCC350 (GenBank EU375803) [23] was used (MCPyV large T [LT]). The forward primer was 5'-AGGTTGACGAGGCCCCTAT-3', and the reverse primer was 5'-TTCCCGAAGCT-GAATCCTC-3' (amplicon size 76 bp). Locked nucleic acid probe 22 was used for MCPyV DNA detection. Thermal cycling consisted of incubation for 2 minutes at 50°C with an initial denaturation for 10 minutes at 95°C followed by 40 cycles of denaturation for 15 seconds at 95°C and annealing for 1 minute at 60°C, as previously described [23]. The ratio of the virus was determined using the signal in the positive MCC sample as a reference. Thresholds were plotted against each standard sample. All reactions of samples and controls were performed in triplicate, and the average is reported. The MCPyV DNA ratio in each sample was determined on the basis of the corresponding standard curves.

2.5. Immunohistochemistry for detection of MCPyV-LT

For the detection of MCPyV-LT antigen expression, IHC staining was performed using monoclonal antibody CM2B4 (mouse monoclonal IgG2b, 200 μg/mL; sc-136172; Santa Cruz Biotechnology, CA), which was generated using the peptide fragment of MCPyV-LT as an immunogen [23]. Four-micrometer LCH sample sections were deparaffinized and rehydrated. Endogenous peroxidase activity was blocked using 3% hydrogen peroxide in methanol for 15 minutes. Antigen retrieval was performed by incubating the sections in citrate buffer (pH 6.0) for 10 minutes at 95°C. The sections were incubated with CM2B4 (diluted at 1:100) overnight at 4°C and then washed in phosphate-buffered saline. Peroxidase-conjugated goat antimouse IgG was applied as the secondary antibody. Sections were incubated for 30 minutes at room temperature then washed in phosphate-buffered saline. Diaminobenzidine was used as the chromogen.

2.6. Statistical analysis

Comparisons of the values of the MCPyV DNA sequences from patients with LCH-RO+ and those with LCH-RO− were statistically analyzed using Fisher's exact test. The numbers of MCPyV DNA sequences obtained by

Q-PCR of patients with LCH, RLH, and non-LCH dermal disease data were also correlated using Fisher's exact test. Differences between the values were considered statistically significant at $P < .05$.

3. Results

3.1. MCPyV DNA in PBMCs from patients with LCH

The MCPyV DNA sequences were detected in PBMCs from patients with LCH-RO+ in 2 of the 3 analyzed samples, but there were no DNA sequences in any of the 12 samples corresponding to LCH-RO− ($P = .029$). Comparisons of MCPyV DNA sequences in PBMCs of patients with SS-LCH and of patients with MS-LCH did not differ significantly (0/6 versus 2/9; $P = .49$) (Table 1).

3.2. MCPyV DNA sequences in LCH tissues versus tissues of RLH, non-LCH skin diseases, and DLA

The viral loads of MCPyV detected by Q-PCR analysis in LCH tissues are shown in Table 2. MCPyV DNA sequences were detected in 12 of 13 tissue samples from patients with LCH, a significant difference from tissues from RLH patients (0/5; $P = .0007$; Table 3) or DLA patients (5/20; $P = .0007$; Table 4). The numbers of MCPyV DNA sequences in all four LCH tissues from patients younger than 2 years indicated a significant difference from tissues of non-LCH dermal disease patients of the same age (0/11; $P = .0007$), as reported in Tables 2 and 5.

Two tissue samples were obtained at 2 times from patient LCHT3 (Table 2) affected by an LCH lesion located in the epidural space between the fifth and seventh thoracic vertebrae. The MCPyV DNA was not detected in the first specimen that clearly contained LCH cells, whereas the second specimen obtained during a later second operation confirmed the presence of MCPyV DNA sequences. Comparatively, the two fragments obtained from patient LCHT7, the first from the femur and the second from the rib, both demonstrated the presence of MCPyV DNA sequences (Table 2).

3.3. MCPyV-DNA sequences in microdissected LCH lesions in comparison with microdissected DLA tissues

The microdissected areas containing S100-positive cells showed MCPyV DNA sequences by Q-PCR analysis in four of the five LCH samples (Table 6) and in both DLA samples (Table 7). Of note, MCPyV DNA sequences were not detected in LCH cells from patient LCHT12, although MCPyV DNA was detected in microdissected epidermis that included S100-positive LCs (viral load = 0.0006 copies/cell). Comparatively, the microdissected areas containing S100-negative lymphoid cells within the LCH or DLA tissues did not contain MCPyV DNA sequences in any of the 5 LCH samples or the two DLA samples analyzed.

3.4. IHC staining for MCPyV-LT

Positive cytoplasmic or nuclear immunoreactivity was observed in LCH cells corresponding to tissues where a higher viral load was detected by Q-PCR (2/13; LCHT7 and LCHT12; Fig.) compared with absent immunoreactivity in LCH tissues with low viral loads (see Table 2).

Table 1 Clinical characteristics and amounts of MCPyV-DNA in PBMCs of patients with Langerhans cell histiocytosis

Patient	Age/Sex	Subtype	Distribution	Risk organ	Viral load (Q-PCR)
LCHB1	0 mo/F	MS	Skin, BM	+	+ (0.0003)
LCHB2	3 mo/M	MS	Skin, thymus, oral mucosa, liver, BM, LN	+	+ (0.001)
LCHB3	1 y 4 mo/M	MS	Skin, liver, spleen, lung	+	−
LCHB4	1 y/M	MS	Bone, orbit	−	−
LCHB5	1 y 2 mo/F	MS	Skin, bone	−	−
LCHB6	1 y 4 mo/M	MS	Skin, bone	−	−
LCHB7	2 y/M	MS	Skin, LN	−	−
LCHB8	3 y/M	MS	Bone, LN	−	−
LCHB9	12 y/F	MS	Skin, CNS	−	−
LCHB10	3 mo/M	SS	Skin	−	−
LCHB11	1 y 7 mo/F	SS	Bone	−	−
LCHB12	2 y/M	SS	Bone	−	−
LCHB13	4 y/F	SS	Bone	−	−
LCHB14	6 y/M	SS	Bone	−	−
LCHB15	7 y/M	SS	Bone	−	−

NOTE. Median age of 15 patients was 1 y 7 mo (range 0 mo to 7 y). Viral load is shown as copies per cell in cases positive for MCPyV.

Abbreviations: BM, bone marrow; CNS, central nervous system; LCHB, Langerhans cell histiocytosis blood; LN, lymph node; MS, multisystem LCH; SS, single-system LCH; +, involvement of at least one high-risk organ or viral load detected; −, no involvement of high-risk organ or no viral load detected.

Table 2   Clinical characteristics and amounts of MCPyV in tissues of patients with Langerhans cell histiocytosis

Patient	Age/sex	Subtype	Risk organ	Biopsy site	Q-PCR (Viral Load)	MCPyV-LT (CM2B4)
LCHT1	86 y/F	SS	–	Bone	+ (0.006)	–
LCHT2	9 mo/F	SS	–	Oral mucosa	+ (0.002)	–
LCHT3	52 y/M	SS	–	Soft tissue	+ (0.002)	–
LCHT4	14 y/M	SS	–	Bone	+ (0.002)	–
LCHT5	5 mo/F	SS	–	Skin	+ (0.005)	–
LCHT6	41 y/F	SS	–	Pituitary	+ (0.002)	–
LCHT7	21 y/M	SS	–	Bone	+ (0.027)	+
LCHT8	6 y/F	MS	–	Bone	+ (0.006)	–
LCHT9	2 y/F	MS	–	Bone	–	–
LCHT10	7 y/F	MS	–	Soft tissue	+ (0.0001)	–
LCHT11	39 y/F	MS	–	Skin	+ (0.002)	–
LCHT12	1 y/F	MS	+	Skin	+ (0.033)	+
LCHT13	6 mo/F	MS	–	Skin	+ (0.003)	–

NOTE. Median age of SS-LCH patients (n = 7) was 22 y (range, 5 mo to 86 y). Median age of MS-LCH patients (n = 6) was 4 y (range, 6 mo to 39 y). Abbreviations: CM2B4, immunostaining of MCPyV large T antigen in LCH cells; LCHT, Langerhans cell histiocytosis tissue; MS, multisystem LCH; SS, single-system LCH; +, involvement of at least one high-risk organ or viral load detected; –, no involvement of high-risk organ or no viral load detected.

4. Discussion

Our previous data indicated that Q-PCR was the most sensitive method for the detection of MCPyV, superior to single PCR and immunohistochemistry staining [19,23]. The Q-PCR for MCPyV-LT also was more sensitive than immunohistochemistry using the CM2B4 antibody (see Table 2). In this report, we describe the presence of MCPyV DNA sequences in two blood samples (see Table 1) as well as in four LCH tissues samples obtained from children younger than 2 years (Table 2). The viral DNA load in blood samples ranged from 30 to 100 molecules per 100 000 cells (0.0003 to 0.001 per cell). No significant differences in the numbers of MCPyV DNA sequences were observed between patients with SS-LCH and those with MS-LCH (Table 1). Concerning the LCH tissues, MCPyV DNA sequences were detected in microdissected areas containing S100-immunoreactive cells in four of the five LCH samples and in both analyzed DLA samples. In contrast, the microdissected areas containing lymphoid cells non-reactive with the anti-S100 antibody did not show MCPyV DNA sequences. Remarkably, a viral DNA load of 0.0006 copies/cell was detected in microdissected areas of the epidermal

layer, which contained S100-positive LCs (see Table 6, patient LCHT12).

MCPyV was frequently detected in the skin of healthy individuals [19,21]. Surprisingly, buffy coats of healthy adult blood donors, which were examined for MCPyV DNA tag sequences, showed a prevalence of 22%, with viral loads ranging from 10 to 100 molecules per 100 000 cells (0.0001 to 0.001 per cell) [26]. As LCs capture foreign antigens in the epidermal layer and migrate toward the lymph nodes,

Table 4   Clinical characteristics and lesional MCPyV data of patients with DLA

Patient	Age (y)/sex	Q-PCR (Viral load)
DLA1	66/F	+ (0.002)
DLA2	54/M	–
DLA3	81/M	+ (0.004)
DLA4	58/M	+ (0.001)
DLA5	63/M	+ (0.001)
DLA6	79/F	+ (0.006)
DLA7	66/M	–
DLA8	65/F	–
DLA9	86/M	–
DLA10	74/M	–
DLA11	35/M	–
DLA12	30/F	–
DLA13	72/F	–
DLA14	87/M	–
DLA15	39/M	–
DLA16	81/M	–
DLA17	73/M	–
DLA18	43/M	–
DLA19	39/M	–
DLA20	68/M	–

NOTE. All biopsies were of lymph nodes. Median age of patients (n = 20) was 66 y (range, 30-87 y).

Table 3   Clinical characteristics and MCPyV in tissues of patients with RLH

Patient	Age (y)/sex	Biopsy site	Q-PCR
RLH1	72/F	Lung	–
RLH2	79/F	Lung	–
RLH3	62/M	Nasal cavity	–
RLH4	32/F	Lymph node	–
RLH5	75/F	Lymph node	–

NOTE. Median age of patients (n = 5) was 72 y (range, 32-79 y).

Table 5 Clinical characteristics and lesional MCPyV data of patients younger than 2 years with non-LCH dermal diseases

Patient	Age/sex	Diagnosis	Q-PCR
S1	1 y 4 mo/F	Nevocellular nevus	−
S2	1 y 6 mo/F	Nevocellular nevus	−
S3	8 mo/F	Xanthogranuloma	−
S4	1 y 6 mo/F	Dermoid cyst	−
S5	1 y 9 mo/M	Blue nevus	−
S6	1 mo/F	Nevocellular nevus	−
S7	1 y 3 mo/F	Nevus sebaceous	−
S8	1 mo/F	Xanthogranuloma	−
S9	1 y 4 mo/F	Dermoid cyst	−
S10	1 y 3 mo/F	Dermatitis	−
S11	1 y 4 mo/F	Nevocellular nevus	−

NOTE. All biopsies were from skin. Median age of patients (n = 11) was 1 y 4 mo (range, 1 mo to 1 y 9 mo).

Table 7 Detection of MCPyV DNA by Q-PCR in whole DLA samples and microdissected S100+ or S100− DLA lesions

Patient	Q-PCR (viral load)	Q-PCR (Microdissection)	
		S100+ (viral load)	S100−
DLA3	+ (0.004)	+ (0.0003)	−
DLA4	+ (0.001)	+ (0.001)	−

detection of MCPyV DNA sequences in both whole (25%; see Table 4) and microdissected DLA tissues (Table 7) suggest that LCs behave as a reservoir for MCPyV in an asymptomatic state and that LCs can transfer the MCPyV DNA from the epidermal layer to lymph nodes.

In patients affected by LCH, antibodies against MCPyV viral proteins (VP) were not detected by enzyme-linked immunoassay in patients younger than 2 years, compared with an incidence of 40% in patients 2 to 5 years of age, about 50% in patients 6–50 years, and 80% in patients older than 50 years [27]. Conversely, in a large seroepidemiologic study, Kean and coworkers [28] showed that about 20% (1–5 years old), 30% (6–10 years), 40% (11–70 years), and 60% (above 70 years) of the healthy population carries anti-MCPyV VP-1 antibodies. Although LCs seem to provide a sanctuary for MCPyV instead of inducing host resistance, as happens with several viruses [16,29], virtually transformed LCH cells may produce intense tissue overreaction and symptoms.

Considering our data, ie, the presence of MCPyV DNA in 4 samples of LCH tissue in patients younger than 2 years (Table 2) together with the previously published seroprevalence of MCPyV in a both healthy population between 1 and 5 years of age [28] and LCH patients younger than 2 years [27] and the absence of viral sequences in non-LCH skin lesions (Table 5), the primary

infection with MCPyV may play a significant pathogenic role in LCH. Thus, the primary infection with MCPyV at the onset of LCH might be related to a disease with severe progression in comparison with a milder course of the disease with onset in the carrier state.

With respect to the presence of other pathogenic infectious agents, Epstein-Barr virus [30], human cytomegalovirus [31], and human herpesvirus 6 [32] have been found in patients affected by LCH. However, at present, they are regarded as bystanders in LCH lesions according to case-controlled seroepidemiologic studies and in situ hybridization analysis [16,33]. In this regard, our data suggest the presence of MCPyV in LCH tissue lesions, especially in patients younger than 2 years (100%; Table 2), excluding the occasional viral infection. In this context, the presence of MCPyV DNA was reported in the blood of a 53-year-old recipient of a renal allograft and a 75-year-old patient with chronic psoriasis and MCC [34]. Mertz and colleagues [34] reported that CD14+ activated monocytes might be a reservoir of MCPyV in the blood and that these cells can spread the inflammatory reactions to various locations in the body. Presumably, LCH cells that currently show elevated numbers of CD14 molecules may also disseminate granulomatous lesions in patients affected by LCH with high-risk organ involvement [35].

5. Conclusion

This is to our knowledge the first report of a relation between MCPyV infection and LCH. We suggest that MCPyV triggers an inflammatory process associated with LCH activity and subtype. The frequent but lower viral loads

Table 6 Detection of MCPyV-DNA by Q-PCR of whole LCHT samples and microdissected S100+ or S100− from LCH lesions

Patient	Subtype	Biopsy site	Viral load (Q-PCR)	Q-PCR (Microdissection)	
				S100+ (Viral load)	S100−
LCHT1	SS	Bone	+ (0.006)	+ (0.02)	−
LCHT3	SS	Soft tissue	+ (0.002)	+ (0.0006)	−
LCHT10	MS	Soft tissue	ND	+ (0.0001)	−
LCHT12	MS	Skin	+ (0.033)[a]	−	(+)
LCHT13	MS	Skin	+ (0.003)	+ (0.001)	−

NOTE. MCPyV-DNA was detected in microdissected epidermal layers, which included S100-positive Langerhans cells (viral load 0.0006).
Abbreviations: MS, multisystem LCH; ND, not done; SS, single-system LCH.
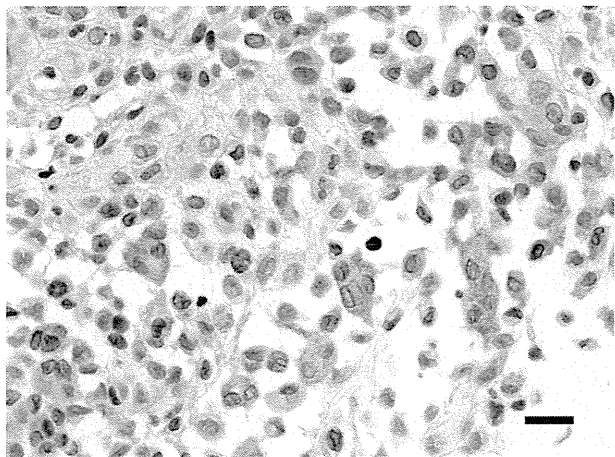
Fig. Immunoreactivity for Merkel cell polyoma virus large T-antigen using monoclonal antibody CM2B4 in multisystem Langerhans cell histiocytosis tissue (LCHT7). Scale bar, 20 μm.

detected by Q-PCR and low positive immunoreactivity rate using the anti-MCPyV-LT antibody in 2 of 13 of LCH tissue samples suggest that development of LCH is more a reactive rather than a neoplastic process, which may be relevant to MCPyV infection. We propose that LCH subtypes are defined by abnormal immunoreactivity against the MCPyV pathogen with an underlying oncogenic capacity. These data open novel possibilities for using antiviral molecules for therapeutic interventions in patients affected by LCH.

Acknowledgment

References

[1] Willman CL, Busque L, Griffith BB, et al. Langerhans'-cell histiocytosis (histiocytosis X)—a clonal proliferative disease. N Engl J Med 1994;331:154-60.

[2] Yu RC, Chu C, Buluwela L, Chu AC. Clonal proliferation of Langerhans cells in Langerhans cell histiocytosis. Lancet 1994;343:767-8.

[3] Badalian-Very G, Vergilio JA, Degar BA, et al. Recurrent BRAF mutations in Langerhans cell histiocytosis. Blood 2010;116:1919-23.

[4] Donadieu J, Egeler RM, Pritchard J. Langerhans cell histiocytosis: a clinical update. In: Weitzman S, Egeler RM, editors. Histiocytic Disorders of Children and Adults. Cambridge, UK: Cambridge University Press; 2005. p. 95-129.

[5] Hamre M, Hedberg J, Buckley J, et al. Langerhans cell histiocytosis: an exploratory epidemiologic study of 177 cases. Med Pediatr Oncol 1997;28:92-7.

[6] Finn LS, Jaffe R. Langerhans' cell granuloma confined to the bile duct. Pediatr Pathol Lab Med 1997;17:461-8.

[7] Kaplan KJ, Goodman ZD, Ishak KG. Liver involvement in Langerhans' cell histiocytosis: a study of nine cases. Mod Pathol 1999;12:370-8.

[8] Coury F, Annels N, Rivollier A, et al. Langerhans cell histiocytosis reveals a new IL-17A-dependent pathway of dendritic cell fusion. Nat Med 2008;14:81-7.

[9] Allen CE, McClain KL. Interleukin-17A is not expressed by CD207(+) cells in Langerhans cell histiocytosis lesions. Nat Med 2009;15:483-4 [author reply 4-5].

[10] Peters TL, McClain KL, Allen CE. Neither IL-17A mRNA nor IL-17A protein are detectable in Langerhans cell histiocytosis lesions. Mol Ther 2011;19:1433-9.

[11] Murakami I, Morimoto A, Oka T, et al. IL-17A receptor expression differs between subclasses of Langerhans cell histiocytosis, which might settle the IL-17A controversy. Virchows Arch 2013;462: 219-28.

[12] Ryzhakov G, Lai CC, Blazek K, To KW, Hussell T, Udalova I. IL-17 boosts proinflammatory outcome of antiviral response in human cells. J Immunol 2011;187:5357-62.

[13] Ryzhakov G, Blazek K, Lai CC, Udalova IA. IL-17 receptor adaptor protein Act1/CIKS plays an evolutionarily conserved role in antiviral signaling. J Immunol 2012;189:4852-8.

[14] Murakami I, Oka T, Kuwamoto S, et al. Tyrosine phosphatase SHP-1 is expressed higher in multisystem than in single-system Langerhans cell histiocytosis by immunohistochemistry. Virchows Arch 2011;459: 227-34.

[15] An H, Hou J, Zhou J, et al. Phosphatase SHP-1 promotes TLR- and RIG-I-activated production of type I interferon by inhibiting the kinase IRAK1. Nat Immunol 2008;9:542-50.

[16] da Costa CET, Annels NE, Egeler RM. The immunological basis of Langerhans cell histiocytosis. In: Weitzman S, Egeler RM, editors. Histiocytic Disorders of Children and Adults. Cambridge, UK: Cambridge University Press; 2005. p. 66-82.

[17] Garabedian L, Struyf S, Opdenakker G, Sozzani S, Van Damme J, Laureys G. Langerhans cell histiocytosis: a cytokine/chemokine-mediated disorder? Eur Cytokine Netw 2011;22:148-53.

[18] Cyster JG. Chemokines and the homing of dendritic cells to the T cell areas of lymphoid organs. J Exp Med 1999;189:447-50.

[19] Matsushita M, Kuwamoto S, Iwasaki T, et al. Detection of Merkel cell polyomavirus in the human tissues from 41 Japanese autopsy cases using polymerase chain reaction. Intervirology 2013;56:1-5.

[20] Tolstov YL, Knauer A, Chen JG, et al. Asymptomatic primary Merkel cell polyomavirus infection among adults. Emerg Infect Dis 2011;17: 1371-80.

[21] Foulongne V, Kluger N, Dereure O, et al. Merkel cell polyomavirus in cutaneous swabs. Emerg Infect Dis 2010;16:685-7.

[22] Feng H, Shuda M, Chang Y, Moore PS. Clonal integration of a polyomavirus in human Merkel cell carcinoma. Science 2008;319: 1096-100.

[23] Kuwamoto S. Recent advances in the biology of Merkel cell carcinoma. HUM PATHOL 2011;42:1063-77.

[24] Kubo A, Nagao K, Yokouchi M, Sasaki H, Amagai M. External antigen uptake by Langerhans cells with reorganization of epidermal tight junction barriers. J Exp Med 2009;206:2937-46.

[25] Jaffe R, Weiss LM, Facchetti F. Tumours derived from Langerhans cells. In: Swerdlow SH, Campo E, Harris NL, et al, editors. WHO Classification of Tumours of Haematopoietic and Lymphoid Tissues. Lyon, France: IARC; 2008. p. 358-60.

[26] Pancaldi C, Corazzari V, Maniero S, et al. Merkel cell polyomavirus DNA sequences in the buffy coats of healthy blood donors. Blood 2011;117:7099-101.

[27] Tolstov YL, Pastrana DV, Feng H, et al. Human Merkel cell polyomavirus infection II: MCV is a common human infection that can be detected by conformational capsid epitope immunoassays. Int J Cancer 2009;125:1250-6.

[28] Kean JM, Rao S, Wang M, Garcea RL. Seroepidemiology of human polyomaviruses. PLoS Pathog 2009;5:e1000363.

[29] Banchereau J, Steinman RM. Dendritic cells and the control of immunity. Nature 1998;392:245-52.

[30] Shimakage M, Sasagawa T, Kimura M, et al. Expression of Epstein-Barr virus in Langerhans' cell histiocytosis. HUM PATHOL 2004;35: 862-8.

[31] Kawakubo Y, Kishimoto H, Sato Y, et al. Human cytomegalovirus infection in foci of Langerhans cell histiocytosis. Virchows Arch 1999;434:109-15.

[32] Leahy MA, Krejci SM, Friednash M, et al. Human herpesvirus 6 is present in lesions of Langerhans cell histiocytosis. J Invest Dermatol 1993;101:642-5.

[33] Jeziorski E, Senechal B, Molina TJ, et al. Herpes-virus infection in patients with Langerhans cell histiocytosis: a case-controlled sero-epidemiological study, and in situ analysis. PLoS One 2008;3:e3262.

[34] Mertz KD, Junt T, Schmid M, Pfaltz M, Kempf W. Inflammatory monocytes are a reservoir for Merkel cell polyomavirus. J Invest Dermatol 2010;130:1146-51.

[35] Geissmann F, Lepelletier Y, Fraitag S, et al. Differentiation of Langerhans cells in Langerhans cell histiocytosis. Blood 2001;97: 1241-8.

Osteopontin Has a Crucial Role in Osteoclast-Like Multinucleated Giant Cell Formation

Yukiko Oh,[1]* Iekuni Oh,[2] Junko Morimoto,[3] Toshimitsu Uede,[3] and Akira Morimoto[1]

[1]Department of Pediatrics, Jichi Medical University School of Medicine, 3311-1, Yakushi-ji, Shimotsuke, Tochigi 329-0498, Japan

[2]Department of Hematology, Jichi Medical University School of Medicine, 3311-1, Yakushi-ji, Shimotsuke, Tochigi 329-0498, Japan

[3]Division of Molecular Immunology, Institute for Genetic Medicine, Hokkaido University, Kita-15, Nishi-7, Kita-ku, Sapporo 060-0815, Japan

ABSTRACT

The osteoclast (OC) is a major player in the pathogenic bone destruction of inflammatory bone diseases such as rheumatoid arthritis and Langerhans cell histiocytosis. Recently, it was shown that immature dendritic cells (iDC) fuse faster and more efficiently than monocytes in forming OC-like multinucleated giant cells (MGCs), and that osteopontin (OPN) is involved in the pathogenesis of inflammatory bone diseases. In this study, we hypothesized that OPN is a key factor for generation of OC-like MGCs from iDCs. We used an in vitro culture system to differentiate iDCs, derived from monocytes obtained from the blood of healthy donors, into OC-like MGCs. We evaluated OPN levels and expression of OPN receptors during the course of differentiation. OPN has an arginine-glycine-aspartic acid (RGD) motif, and protease cleavage reveals a SVVYGLR motif. The concentrations of both full-length and cleaved forms of OPN increased during the course of OC-like MGC formation. Expression of OPN RGD- and SVVYGLR-recognizing receptors also increased at later stages. We analyzed whether blocking OPN binding to its receptors affected OC-like MGC formation. Monocytes treated with OPN siRNA were able to differentiate into iDCs effectively; however, differentiation of these iDCs into OC-like MGCs was significantly reduced. The formation of OC-like MGCs was not significantly reduced by RGD synthetic peptide. By contrast, SVVYGLR synthetic peptide caused a significant reduction. These data suggest that the cleaved form of OPN plays a critical role in driving iDC differentiation into OC-like MGCs in the early phase of differentiation, in an autocrine and/or paracrine fashion. J. Cell. Biochem. 115: 585–595, 2014. © 2013 Wiley Periodicals, Inc.

KEY WORDS: OSTEOPONTIN; OSTEOCLAST; IMMATURE DENDRITIC CELL; MULTINUCLEATED GIANT CELL; INFLAMMATORY BONE DISEASE

Osteoclasts (OC) are bone-resorbing giant polykaryon cells that differentiate from mononuclear macrophage/monocyte-lineage hematopoietic precursors. Upon stimulation by cytokines, such as macrophage colony-stimulating factor (M-CSF) and receptor activator of NF-κB ligand (RANKL), OC precursor cells migrate and attach onto the bone surface. There they fuse with each other to form multinucleated giant cells (MGCs) and mediate bone resorption [Teitelbaum, 2000].

Osteopontin (OPN) plays an important role physiologically in bone remodeling, especially in bone resorption, by modulating OC function [Chellaiah et al., 2003; Standal et al., 2004]. OPN contains the classical cell-binding motif arginine-glycine-aspartic acid (RGD) that binds cell surface RGD-recognizing integrins such as αvβ1, αvβ3, α5β1, and CD44 variant (v) 6 [Hu et al., 1995; Gao et al., 2003]. RGD-recognizing integrins are expressed by a variety of cells including fibroblasts, smooth muscle cells, endothelial cells, epithelial cells, and immune cells [Uede, 2011]. OPN can be cleaved by proteases, including thrombin and plasmin, which exposes a serine-valine-valine-tyrosine-glycine-leucine-arginine (SVVYGLR) motif [Yokosaki et al., 1999]. This motif is recognized by non-RGD-recognizing integrins such as α4β1 expressed by T cells and macrophages, and α9β1 expressed by fibroblasts, neutrophils, macrophages, smooth muscle cells, and OCs [Smith et al., 1996; Green et al., 2001].

OCs play a major role in the pathogenic bone destruction of rheumatoid arthritis (RA) and Langerhans cell histiocytosis (LCH) [Redlich et al., 2002; da Costa et al., 2005]. Recently, it was revealed that immature dendritic cells (iDC) fuse more quickly and efficiently than monocytes to form OC-like MGCs in the inflammatory environment [Rivollier et al., 2004]. This suggests that iDC-derived OCs may be directly involved in the osteolytic lesions observed in inflammatory bone diseases such as RA or LCH. OPN is implicated in the pathogenesis of RA [Yumoto et al., 2002; Yamamoto et al., 2007] and LCH [Prasse et al., 2009; Allen et al., 2010].

Based on these findings, we hypothesized that OPN is a key factor in the formation of OC-like MGCs from iDCs. In this study we found that OPN, particularly after cleavage, plays a critical role in the formation of OC-like MGCs from iDCs in an autocrine and paracrine manner.

MATERIALS AND METHODS

MONOCYTE PURIFICATION AND IDC DIFFERENTIATION

Monocytes and iDCs were defined by the expression of CD14 and CD1a, respectively [Chapuis et al., 1997]. PBMC were obtained from healthy adult volunteer donors. Informed consent was obtained from them. The ethics committee, Jichi Medical University School of Medicine approved this study. A positive selection of CD14$^+$ cells was performed by adding MACS colloidal superparamagnetic microbeads conjugated with monoclonal anti-human CD14 Abs (IgG2a), (Miltenyi Biotec, Tokyo, Japan) to freshly prepared PBMC preparation in MACS buffer according to the manufacture's instructions. Briefly, after incubation of cells and microbeads (15 min at 4°C), cells were washed with MACS buffer, resuspended, and loaded onto the top of the separation column. Trapped CD14$^+$ PBMC were eluted with a sixfold amount of cold MACS buffer. Using flow cytometry, the purity of the CD14$^+$ cells was evaluated at 98.8 ± 0.4%.

Purified monocytes were used to generate monocyte-derived iDCs in vitro, as previously described [Rivollier et al., 2004]. Briefly, monocytes were seeded at 10^6 cells/ml and maintained in RPMI 1640 (Life Technologies, Paisley, UK) supplemented with 10 mM N-2-hydroxyethylpiperazine-N'-2-ethanesulfonic acid (HEPES), 2 mM L-glutamine, 100 U/ml penicillin and 100 μg/ml streptomycin (Life Technologies), 10% heat-inactivated fetal calf serum (FCS; Biological Industries, Beit Haemek, Israel), 50 ng/ml human recombinant (h) granulocyte-macrophage colony-stimulating factor (GM-CSF), and 500 U/ml h IL-4 (PeproTech, Rocky Hill, NJ). After 5 days in culture, more than 90% of the cells were iDCs as assessed by CD1a labeling.

OC-LIKE MGC FORMATION AND TRAP ASSAY

iDCs were seeded at 1,600 cells/mm^2 in 48-well plates, into which a sterilized glass coverslip was placed, in α-minimum essential medium (α-MEM) (Life Technologies) supplemented with 10% FCS, 2 mM L-glutamine, 100 U/ml penicillin, and 100 μg/ml streptomycin in the presence of 25 ng/ml M-CSF and 100 ng/ml RANKL (PeproTech, Rocky Hill, NJ). During the course of differentiation, we harvested culture supernatants and various cells including monocytes, iDCs, and various differential stages of OC-like MGCs at day 4 (OC4), day 8 (OC8), and day 12 (OC12). Tartrate-resistant acid phosphatase (TRAP)

activity, a signature marker for OCs, was assessed using a leukocyte acid phosphatase kit (Sigma–Aldrich) at day 12. Nuclear DNA was stained with 10 μg/ml Hoechst 33342 (Sigma–Aldrich) for 30 min at 37°C and fixed with 15% formol.

SUPPRESSION OF OPN BY RNA INTERFERENCE

Suppression of OPN expression was performed by RNA interference using specific small interfering RNA oligonucleotides (siRNA) (ccaaguaaguccaacgaaaTT). Control siRNA sequence was acucuau-cugcacgcugacTT. siRNAs were transfected into human monocytes or monocyte-derived iDCs using Lipofectamine RNAiMAX (Life Technologies). Transfected monocytes or iDCs were cultured to form OC-like MGCs as described above. The number of OC-like MGCs (TRAP-positive and strictly more than two nuclei) was counted on day 7 of OC differentiation.

INHIBITION OF MGC FORMATION WITH SYNTHETIC PEPTIDES DERIVED OPN INTERNAL SEQUENCE

In order to examine whether the interaction of OPN and its receptors is involved in MGC formation, we used synthetic peptides (RGD and SVVYGLR) to both RGD-recognizing and SVVYGLR-recognizing integrins. RGD and SVVYGLR peptides interfere with the binding of OPN to RGD- and non RGD ($\alpha 4\beta 1$ and $\alpha 9\beta 1$) integrins, respectively [Storgard et al., 1999; Green et al., 2001]. MGCs were differentiated from iDCs, in the presence of 10 μg/ml RGD or RGE (control) peptides (Abbiotec, San Diego, CA), or 1 μg/ml SVVYGLR or GRVLYSV (control) peptides (GenScript, Piscataway, NJ). The number of OC-like MGCs (TRAP-positive and strictly more than two nuclei) was counted on day 7 of OC differentiation.

IMMUNOFLUORESCENCE AND MICROSCOPY

Monocytes and iDC were attached to slide glass by cytospin. Monocytes, iDC and cells cultured on glass coverslips (OC4, OC8, OC12) were first fixed with 4% paraformaldehyde for 30 min at 4°C. The slide glass or the glass coverslips were incubated in normal goat serum for 30 min at 30°C, followed by primary antibody (polyclonal rabbit anti-human OPN antibody (IgG), (Abcam, Cambridge, UK), polyclonal rabbit anti-human CD1a antibody (Sigma–Aldrich, St. Louis, MO), monoclonal mouse anti-human CD44v6 antibody (IgG1), (Leica, Newcastle upon Tyne, UK), monoclonal mouse anti-human $\alpha v\beta 3$ antibody (IgG1), (Hycult Biotech, Uden, The Netherlands), and monoclonal mouse anti-human $\alpha 9\beta 1$ antibody (IgG1), (Abcam) for a further overnight at room temperature. Rabbit IgG (SP137), (Abcam) and mouse IgG1 (MOPC21), (Affinity BioReagents, Golden, CO) was used as substitute isotype control. After washing with PBS, the appropriate secondary antibody (Alexa Fluor 488 goat anti-mouse IgG (H + L), Alexa Fluor 488 goat anti-rabbit IgG (H + L), or Alexa Fluor 555 goat anti-mouse IgG (H + L) (Molecular Probes, Inc., Eugene, OR) was applied for 30 min at 30°C. Nuclear DNA was stained by DAPI (4'-6-diamidino-2-phenylindole). The cells were analyzed using an Olympus AX80 microscope equipped with an 40×/0.85 NA or a 100×/1.35 oil iris NA objective lens, an Olympus DP70 camera, and Olympus DP controller software (Olympus Co. Ltd., Tokyo, Japan). The number of CD1a positive cells and $\alpha 9\beta 1$ positive cells was counted on monocyte, iDC, and day 4, 8, 12 of OC differentiation.

QUANTIFICATION OF IMMUNOFLUORESCENCE

Images collected using the Olympus DP controller software were analyzed for immunofluorescence intensity using Adobe Photoshop Elements, version 11 (Adobe Systems Incorporated, Tokyo, Japan) as follows. Using the magic wand tool in the "Select" menu of Photoshop, the cursor was placed on $\alpha9\beta1$-positive cytoplasm. The tolerance level of the magic wand tool was adjusted so that the entire positive cytoplasm was selected automatically. The mean staining intensity was calculated as follows: intensity score (IS) = mean of brightness of selected cells' red channel score (in arbitrary units, AU) using Adobe Photoshop Elements, version 11 [Murakami et al., 2013].

RELATIVE QUANTITATIVE RT-PCR

Levels of OPN, CD44v6, integrin αv, and integrin $\alpha 9$ mRNA were measured by relative quantitative real-time reverse transcription polymerase chain reaction (RT-PCR) using the 7500 Fast System (Applied Biosystems, Foster City, CA); β-actin was used as an internal standard. Briefly, RNA was isolated from the harvested cells using an RNeasy kit (Qiagen, Hilden, Germany), reverse transcribed, and PCR amplified using a One Step PrimeScript RT-PCR Kit (Takara Bio, Shiga, Japan), with TaqMan Gene Expression Assay primers for human OPN (Hs00959010), integrin αv (Hs00233808), integrin $\alpha 9$ (Hs00979865), CD44v6 (Hs01075854), and β-actin (Hs99999903). Data were analyzed using the $2^{-\Delta\Delta C_t}$ method.

MEASUREMENTS OF THE FULL-LENGTH AND THE CLEAVED FORMS OF OPN IN THE CELL SUPERNATANT

We measured the amounts of the full-length OPN in the cell culture supernatant with human osteopontin ELISA kit (R&D Systems, Minneapolis, MN) and the cleaved forms of OPN with human osteopontin N-half assay kit (IBL, Gunma, Japan), which can specifically measure the N-terminal OPN fragment cleaved by thrombin. N-terminal OPN fragments expose a cryptic epitope, SVVYGLR, which is recognized by $\alpha9\beta1$ integrin. Thus, the presence of high amounts of N-half OPN indicates the involvement of $\alpha9\beta1$ integrin in OC-like MGC differentiation.

FLOW CYTOMETRIC ANALYSIS

We used directly conjugated antibodies, FITC-anti-CD14 (M5E2), PE-anti-CD1a (HI149), FITC-IgG2a (G155-178), and PE-IgG1 (MOPC-21) (BD Pharmingen, Tokyo, Japan). Cells were suspended in PBS supplemented with 10% FCS (FACS buffer) and stained with appropriate concentrations of antibodies for 15 min on ice, then washed with FACS buffer. Cells were analyzed using a BD LSR cytometer and CellQuest software (BD, Tokyo, Japan).

DETERMINATION OF VIABILITY AND APOPTOSIS

For floating cells, we analyzed the proportion of viable and apoptotic cells using flow cytometry. The number of floating cells was counted, cells were suspended in binding buffer (BD Pharmingen, Tokyo, Japan), and cell suspensions were incubated with Annexin V-PE and 7-AAD (BD Pharmingen, Tokyo, Japan) for 15 min at room temperature. Cells were analyzed using a BD LSR Fortessa cell analyzer and FlowJo software (Tree Star, San Carlos, CA). Unstained cells were used as negative controls. Viable cells were defined as double negative for Annexin V and 7-AAD, and apoptotic cells were defined as Annexin V

positive and 7-AAD negative. For analysis of adherent cells, cells cultured on glass coverslips were stained by 0.4% trypan blue to count viable cells. To detect apoptotic cells, terminal deoxynucleotidyl transferase mediated dUTP nick end labeling (TUNEL) stain was performed. Cells were fixed with 4% paraformaldehyde for 30 min at 4°C. The glass coverslips were incubated with permeabilization buffer for 2 min at 4°C, followed by FITC-labeled terminal deoxynucleotidyl transferase (TdT) enzyme for 90 min at 37°C. DNA was stained by DAPI. The cells were analyzed using an Olympus AX80 microscope.

QUANTIFICATION OF CASPASE-3 ACTIVITY

Caspase-3 activity was quantified using an ApoAlert Caspase-3 colorimetric assay kit (Clontech, Tokyo, Japan). This assay uses the spectrophotometric detection of the chromophore p-nitroaniline (pNA) after its cleavage by caspases from the labeled caspase-specific substrates. 1.5×10^5 cells were harvested at each stage (OC1, OC3, and OC7), and resuspended in 50 μl of lysis buffer and incubated for 10 min at 4°C. Cell suspension were centrifuged at 15,000 rpm for 10 min. Twenty-five microliters of the supernatants were added to 25 μl of 2× reaction buffer, and then incubated with caspase-3 substrate, aspartic acid-glutamic acid-valine-aspartic acid (DEVD)-p-nitroaniline (pNA), for 60 min at 37°C. The chromophore pNA was measured at 405 nm in Benchmark Plus microplate reader (BIO-RAD, Tokyo, Japan). We constructed a standard curve for each assay run using pNA in the concentration range of 0–200 μM, and converted optical density of each sample into pNA concentration.

MEASUREMENT OF INTRACELLULAR REACTIVE OXYGEN SPECIES PRODUCTION

Reactive oxygen species (ROS) activity was quantified using an OxiSelect Intracellular ROS assay kit (Cell Biolabs, San Diego, CA). Briefly, 1.5×10^5 cells were harvested at each differentiation stage (Mo, iDC, OC1, OC3, and OC7), and then incubated with 100 μl of 2′, 7′-dichlorodihydrofluorescin diacetate (DCFH-DA) at 37°C for 60 min. Cells were washed twice with PBS, and lysed by cell lysis buffer. Fluorescence was measured at 480 nm excitation/530 nm emission in Wallac 1420 ARVO MX (Perkin Elmer, Yokohama, Japan). We constructed a standard curve for each assay run using 2′, 7′-dichlorodihydrofluorescein (DCF) in the concentration range of 0–10 μM, and converted fluorescence intensity into DCF concentration.

INHIBITION OF ROS GENERATION

We used diphenyleneiodonium chloride (DPI) (Enzo Life Sciences, Lausen, Switzerland) or N-acetyl-L-cysteine (NAC) (Sigma–Aldrich) as ROS inhibitors. DPI was dissolved in Dimethyl sulfoxide (DMSO). NAC was dissolved in α-MEM, and pH was adjusted to 7.4 by the addition of NaOH. Monocytes or iDCs were incubated with 100 nM DPI or 20 mM NAC for 60 min at 37°C, and washed twice with medium. Pretreated monocytes were cultured with GM-CSF and IL-4 for 5 days, and pretreated iDCs were cultured with M-CSF and RANKL for 7 days.

STATISTICAL ANALYSIS

The paired t-test was used to analyze the difference between groups; $P < 0.05$ was considered significant. All error bars in this study represent the standard error mean of the mean (SEM). Statistical analyses were performed using Microsoft Excel software.

OPN PRODUCTION IS INCREASED DURING THE COURSE OF OC-LIKE MGC FORMATION FROM iDCs

The production of OPN mRNA and protein was investigated over the course of OC-like MGC formation from iDCs in vitro. First, we obtained monocytes from the blood of healthy adult volunteer donors and from them generated iDCs and then OC-like MGCs using an in vitro culture system (Fig. 1A). During the course of differentiation, we harvested culture supernatants and various cells including monocytes, iDCs, and various differential stages of OC-like MGCs at day 4 (OC4), day 8 (OC8), and day 12 (OC12). Monocytes had no detectable
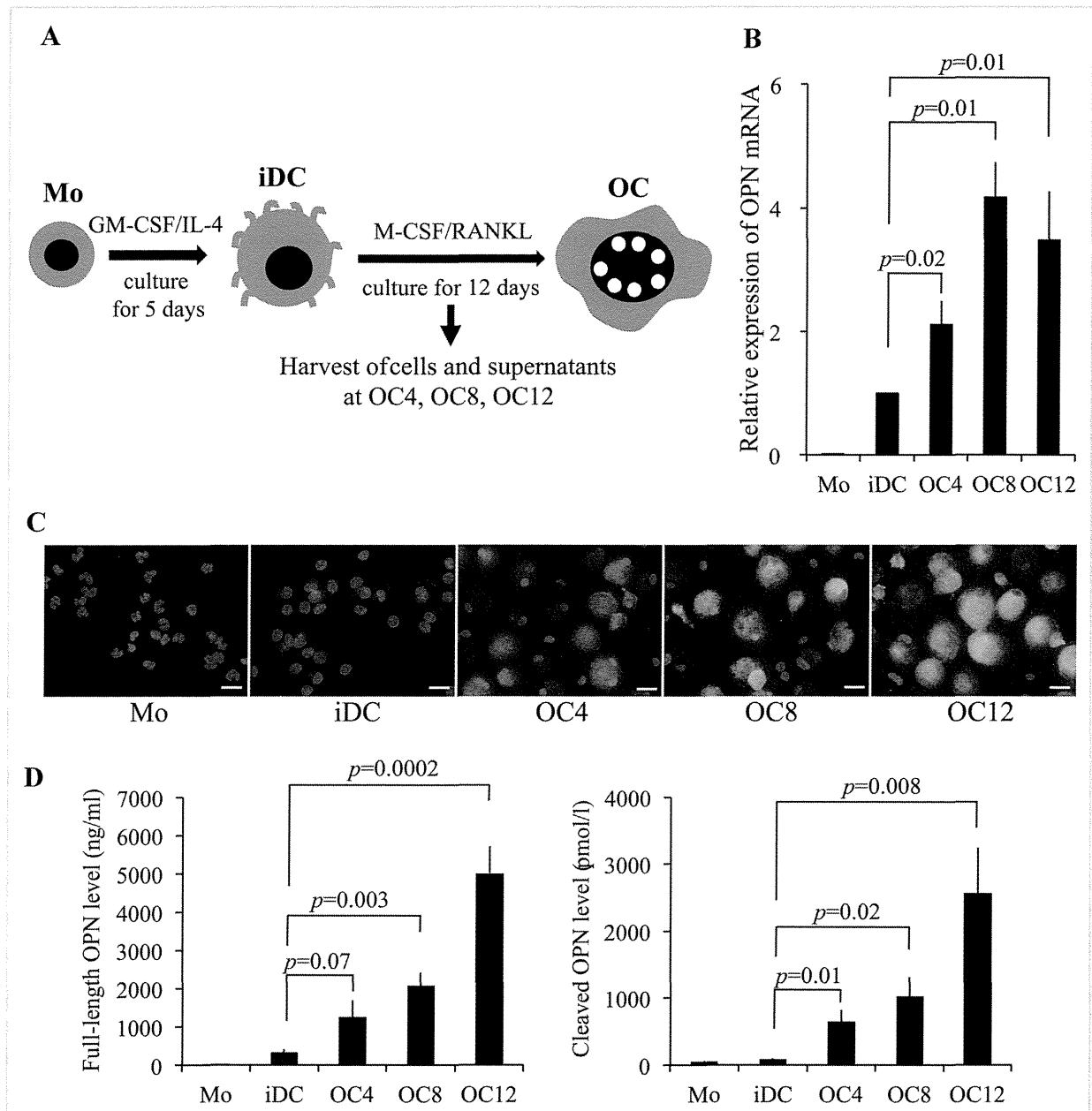

Fig. 1.   OPN production in the course of OC-like MGC formation from iDCs in vitro. A: Schema of experimental design. Monocytes were purified from the peripheral blood of healthy adult volunteer donors. Monocyte-derived immature dendritic cells were generated in vitro by culturing for 5 days with GM-CSF/IL-4. Osteoclasts were generated in vitro by culturing iDCs for 12 days with M-CSF/RANKL. Cells and supernatants were harvested from the starting population of monocytes, the resultant iDCs, and OC-like MGCs on day 4, day 8, and day 12 of culture. B: OPN mRNA expression measured by relative quantitative RT-PCR (data shown are the mean of experiments with cells from five donors). Error bars represent mean ± SEM. C: Immunofluorescence staining with anti-OPN antibody (green) and DAPI (blue) performed on Mo, iDC, OC4, OC8, and OC12. Bars: 20 μm. D: Full-length and cleaved OPN in the cell culture supernatants of OC differentiation from iDCs (independent experiments with cells from eight donors). Error bars represent mean of the eight experiments ± SEM. GM-CSF, granulocyte-macrophage colony-stimulating factor; iDC, immature dendritic cell; M-CSF, macrophage colony-stimulating factor; MGC, multinucleated giant cell; Mo, monocyte; OC: osteoclast; OC4, OC-like MGCs on day 4; OC8, OC-like MGCs on day 8; OC12, OC-like MGCs on day 12; OPN, osteopontin; RANKL, receptor activator of NF-κB ligand; siRNA, small interfering RNA.